OCT 26 2004

REPORT DOCUMENTATION PAGE

Form Approved
OMB No. 0704-0188

Public reporting burden for this collection of information is estimated to average 1 hour per response, including the time for reviewing instructions, searching existing data sources, gathering and maintaining the data needed, and completing and reviewing the collection of information. Send comments regarding this burden estimate or any other aspect of this collection of information, including suggestions for reducing this burden, to Washington Headquarters Services, Directorate for Information Operations and Reports, 1215 Jefferson Davis Highway, Suite 1204, Arlington, VA 22202-4302, and to the Office of Management and Budget, Paperwork Reduction Project (0704-0188), Washington, DC 20503.

1. AGENCY USE ONLY *(Leave blank)*	2. REPORT DATE	3. REPORT TYPE AND DATES COVERED
	25.Oct.04	THESIS

4. TITLE AND SUBTITLE
VIBRATION TESTINGOF THE NASA CONSTELLATION X SPECTROSCOPY X-RAY TELESCOPE REFLECTORS

5. FUNDING NUMBERS

6. AUTHOR(S)
2D LT CARLSON ANDREW J

7. PERFORMING ORGANIZATION NAME(S) AND ADDRESS(ES)
THE GEORGE WASHINGTON UNIVERSITY

8. PERFORMING ORGANIZATION REPORT NUMBER
CI04-649

9. SPONSORING/MONITORING AGENCY NAME(S) AND ADDRESS(ES)
THE DEPARTMENT OF THE AIR FORCE
AFIT/CIA, BLDG 125
2950 P STREET
WPAFB OH 45433

10. SPONSORING/MONITORING AGENCY REPORT NUMBER

11. SUPPLEMENTARY NOTES

12a. DISTRIBUTION AVAILABILITY STATEMENT
Unlimited distribution
In Accordance With AFI 35-205/AFIT Sup 1

12b. DISTRIBUTION CODE

13. ABSTRACT *(Maximum 200 words)*

DISTRIBUTION STATEMENT A
Approved for Public Release
Distribution Unlimited

20041102 038

14. SUBJECT TERMS

15. NUMBER OF PAGES
63

16. PRICE CODE

17. SECURITY CLASSIFICATION OF REPORT	18. SECURITY CLASSIFICATION OF THIS PAGE	19. SECURITY CLASSIFICATION OF ABSTRACT	20. LIMITATION OF ABSTRACT

BEST AVAILABLE COPY

ABSTRACT

This thesis was written with four purposes in mind:

- *Understand at what g-level the glass will fracture in the current mounting scheme.* The data will help the Mechanical Systems Engineering Team of the SXT portion of the Con-X program at NASA-GSFC determine whether the reflectors will survive the loads generated in a launch environment. Design improvements are then considered.
- *Provide data by which to correlate the design team's analytical models.* The data collected by the vibration test will be implemented to fix and improve the current prediction models. Accurate models allow for more simulation and less physical testing, which could possibly save time and money.
- *Create a baseline by which to compare other mounting schemes.* The data collected in the current mounting scheme will be used as a comparison to other mounting schemes. Various materials that interface the glass reflectors and the titanium struts may be effectively compared to determine the optimal mounting configuration.
- *Develop a vibration test that is low cost, but extremely useful to the program.* December 2003 marked severe budget cuts to the NASA Constellation X program. This in turn forced the Mechanical Systems Engineering Team to cancel a previously schedule vibration test that was estimated to cost $30,000. This new series of tests will cost $1,000 for unlimited use of the vibration facility for one year and some minor costs for machining and buying of the test hardware.

This thesis will be made available to the members of the NASA Con-X program and engineering students at The George Washington University.

VIBRATION TESTING OF THE NASA CONSTELLATION X SPECTROSCOPY X-RAY TELESCOPE REFLECTORS

By

Andrew Carlson

B.S. in Aeronautical Engineering, May 2003, United States Air Force Academy

A Thesis submitted to

The Faculty of

The School of Engineering and Applied Science

of The George Washington University in partial satisfaction

of the requirement for the degree of Master of Science.

24 September, 2004

Thesis directed by

Shahram Sarkani

Professor of Engineering Management and Systems Engineering

ACKNOWLEDGEMENT AND DEDICATION

This thesis is dedicated to the members of the NASA Constellation X Spectroscopy X-Ray Telescope Mechanical Systems Engineering Team. I would like to thank the members of the Mechanical Systems Engineering Team for their help in design, manufacturing, and vibration. The main members of this team include Jeffrey Stewart (GSFC-543), Chris Kolos (GSFC-547), Bobby Nanan (Swale), Burt Squires (Swale), Janet Squires (Swale), and William Davis (Harvard-SAO). The strength testing and analysis of the D-263 completed by Dr. Charles He (Swale) and Dr. Len Wang (Swale) has proved very useful. Dr. William Zhang (GSFC-662) and his team provided the samples to complete this test and also gave incite on previous materials studied (prior to the selection of D263). Dr. Arun Varshneya of Alfred University provided incite on the fundamentals of using Weibull statistics. Eliezer Ahronovich (GSFC-573) provided great advice in the design of the base plate and vibration fixture regarding bolt and accelerometer placement. Noble Jones (GSFC-573) provided instruction on using the vibration facility and monitored the testing of our article. I would also like to thank Professor Shahram Sarkani of The George Washington University for his guidance, encouragement, and oversight in organizing and completing this thesis.

The views expressed in this article are those of the author and do not reflect the official policy or position of the United States Air Force, Department of Defense, or the U.S. Government

TABLE OF CONTENTS

LIST OF FIGURES

LIST OF TABLES

LIST OF ACRONYMS

AFM	Atomic Force Microscopy
CCD	Charge Coupled Device
Con-X	Constellation X
CTE	Coefficient of Thermal Expansion
DVC	Digital Vibration Controller
ELV	Expendable Launch Vehicle
FEA	Finite Element Analysis
FEM	Finite Element Model
FMA	Federal Marketing Associates
FS	Factor of Safety
GEVS	General Environmental Verification Specification
GSFC	Goddard Space Flight Center
H	Hyperbolic (Secondary)
HXT	Hard X-Ray Telescope
LDS	Ling Dynamic Systems
L2	Lagrange Point 2
MS	Margin of Safety
NASA	National Aeronautics and Space Administration
OAP	Optical Pathfinder Assembly
P	Primary (Parabolic)
RFC	Reflection Focal Plane Camera
RGS	Reflection Grating Spectrometer

RMS	Root Mean Squared
S	Secondary (Hyperbolic)
SAO	Smithsonian Astrophysical Observatory
SRC	Spectroscopy Readout Camera
STS	Space Transportation System
SXT	Spectroscopy X-Ray Telescope
T	Temperature
TLL	Test Limit Load
TRIP	Technology Readiness and Implementation Plan
XMS	X-Ray Microcalorimeter Spectrometer
ZOC	Zero Order Camera

GLOSSARY

Acoustic Loads	- Forces caused by the engine generated noise of the launch vehicle and by variations in pressure during launch.
Delta	- Change in.
Fatigue	- The weakening of a material (in this case glass) by the time under stress; influenced by many other variables such as ambient humidity, material composition, and the abrasion, thermal and atmospheric history of the glass.
Fundamental Frequency	- The natural frequency of an object, also referred to as the resonance of the test article.
Glass Strength	- Based on the number and types of defects present. Not an intrinsic property of glass due to the large scatter in failure data; dependent upon many variables such as treatment, manufacturing process, handling, and humidity. It is usually measured in ksi or MPa.
Glass Substrate	- See mirror.
High Frequency	- Frequency range from 150 to 2000 Hz covered in a sine sweep.
Hyperbolic Reflector	- The secondary reflector. X-rays reflect off of the secondary to the detectors. It has a shorter focal length than the parabolic reflector.
Low Frequency	- Frequency range from 0 to 150 Hz covered in a sine sweep.
Mirror	- Constellation X reflector. Also referred to as a glass substrate or reflecting mirror.

Parabolic Reflector	- The primary reflector. X-rays reflect off of the primary mirror to the hyperbolic mirror. It has a longer focal length than the hyperbolic reflector.
Primary Reflector	- See Parabolic Reflector.
Replication	- NASA's process of taking a formed reflector and placing it on a gold sputtered precision mandrel under vacuum in an attempt to gain a highly precise gold surface finish.
Reflector	- See Mirror.
Secondary Reflector	- See Hyperbolic Reflector.
Sine Burst	- Vibration test used to verify the structural integrity of a spacecraft component or in the case of destructive testing, to determine the failure point; also known as shock testing.
Sine Sweep	- Vibration test used to search for fundamental frequencies and modal information of a test article; usually associated with a low acceleration (<1 gn).
Slumping	- The process of heating a flat glass sheet in an oven to a point where it will match the shape of the forming mandrel.
Structural Loads	- Mechanically induced forces into and throughout the spacecraft structure, usually greatest during launch.

CHAPTER 1

INTRODUCTION

Constellation X is a state of the art X-Ray telescope that will seek to deliver detailed information on X-Ray associated phenomenon in space. This revolutionary, cutting edge system will allow scientists to study black holes, hot intergalactic medium and celestial events such as supernovas. In order to make this program a reality, the Constellation X team must overcome some stout challenges. One of these challenges is the mounting and precision alignment of 16,000, 400-micron thick, glass optical reflectors. The Constellation X SXT Mechanical Engineering Team is responsible for determining a mounting method for the optics that will allow the spacecraft to survive the harsh loading of the launch environment.

In order to solve the issue of determining an optimized mounting scheme, the design team must fully understand the material properties of the reflectors, which are formulated from Schott D-263 borosilicate glass. In addition to determining the material's strength for input into analytical models, the design team is challenged to understand how the ceramic will behave in a dynamic environment. The launch environment introduces low and high frequency structural loads and high frequency acoustic loads on spacecraft mounted in a launch configuration. These loads may result in the catastrophic failure of a spacecraft and mission if not properly studied, modeled, and tested.

In the fall of 2003, a vibration test was planned for Optical Assembly Pathfinder (OAP) 2, which consists of two mirror substrates aligned and mounted, as they would be for flight. Unfortunately, the Constellation X program suffered from significant budget cuts introduced during December 2003 and this test was cancelled. In order to continue to operate under the new monetary constraints, the project team developed a means to complete the dynamic testing in a

much cheaper, yet effective fashion. The cheaper method of dynamic testing is the primary focus of this thesis.

In order to complete this test, the Con-X SXT Mechanical Engineering Team designed and manufactured a test fixture and associated hardware. It is clear that without the use of a laser-vibrometer and high tech vibration facilities, the data would be less accurate, but still extremely useful in understanding the behavior of the reflectors in the launch configuration. The goals of the test are to understand at what g-level the glass will fracture in the current mounting scheme, to provide data by which to correlate the analytical models, to create a baseline by which to compare other mounting schemes, and to develop a relatively low cost vibration test.

1.1 Review of Literature

A number of documents, meetings, and general conversations proved useful in compiling this thesis. Prior to discussing the literature referenced in this document, it is important to recognize the members of the Constellation X SXT Mechanical Engineering Team (listed in the acknowledgement section) who have provided the analysis, mechanical drawings, and advice used in this thesis. The vibration testing was a team effort. It is important to note that many of the mechanical drawings referenced in other sources and directly throughout the paper are the work of the team designer, Bobby Nanan. Similarly Janet Squires [19] completed much of the analysis, which was referenced in another document and directly referenced in the Problem Statement section. Jeffrey Stewart and Burt Squires provided significant oversight and advice to the efforts. Chris Kolos machined the various parts and William Davis provided thermal analysis of the vibration fixture. All other members of the team played key roles and provided invaluable incite to this project.

The Constellation X-ray Mission TRIP (Technology Readiness and Implementation Plan) Site Visit Briefing [1] provides the purpose of the mission and drawings depicting the overall launch profile. It gives systems level analysis into the design of the telescope. The NASA website, *Constellation X Comparison of Constellation Spectrometer Effective Area with Previous Missions* [2] provided information on the effective area of Constellation X. The website also depicts the *Constellation X Reference Design*, [3] which provides a systems level view of the telescope.

The *SXT FMA Industry Study Pre-Bidder's Conference* [4] shows a functional decomposition of the telescope and explains the reflection and detection of the x-rays. It also contains a drawing depicting the parabolic and hyperbolic modules.

The *Technology Spectroscopy X-Ray Telescope* [5] explains the science behind the Wolter x-ray concept.

The presentation organized by Burt Squires [6] with inputs from the Con-X SXT Mechanical Engineering Team and drawings from Bobby Nanan (Swales) shows how the reflectors are mounted in a sub-module configuration.

The test plan presented by Pilar Joy [7] and the *SXT FMA Industry Study Pre-Bidder's Conference* [4] explains Dr. William Zhang's replication process. Dr. Zhang provided a tour of his facilities and guidance of the replication process and associated issues. Dr. Zhang also explained the history of materials that were examined for use as reflectors and how he settled upon Schott D263 as the most suitable material. He made the point that a brittle material is needed as it maintains its shape better than ductile materials of similar dimensions.

Bansal [8] gives a detailed explanation of the general properties of glass. He also provides incite into how glass behaves in certain environments and how these environmental

factors influence its strength. Villani [9] states the importance of Weibull statistics in the analysis of glass strength and the associated scatter of data. Varshneya [10] provides the equations which are used in analysis. Dr. Varshneya also explained that software is used to determine the Weibull modulus and the normalizing stress parameter.

The D263 properties were provided by the Schott [11] website. Charles He [12,13], the author of two presentations conducts a variety of strength tests. The results of these tests are vital to the analysis performed by Janet Squires as they define the strength that is inputted into the models. His testing has also started to hone in on how defects are introduced during glass processing. His research is extremely important and directly applies to explanation of the vibration testing results.

Chung [14] describes the type of forces that are introduced on a payload by the launch vehicle. The *General Environmental Verification Specification (GEVS) for STS and ELV Payloads, Subsystems, and Components, Revision A* [15] explains the vibration test standards and techniques. Branstetter [16] demonstrates the importance of establishing the excitation and structural characteristics of a system. Chen [17] runs through a vibration test where the focus is on a sinusoidal sweep. Barnes [18] provides a detailed explanation of conducting a sine burst test.

1.2 Chapter Summaries

In order to fully understand and appreciate the purpose of the test, it is important to understand the mission of Constellation X. Chapter 2 of this thesis will provide a decomposed look at the mission and spacecraft design. It will discuss glass properties and specifically the properties of Schott D-263. It will delve into glass strength, which has a direct effect on the survivability of the material in a dynamic environment. The Background will review analytical

studies conducted on the current mounting scheme and discuss the theory of vibrations, which are applicable to this particular testing. Chapter 3 will discuss the goals of the test and what the mechanical team would like to accomplish. It will also discuss the test equipment to include the vibration table, controller, and other hardware. This portion will explain the test plan, procedures, and setup. Chapter 4 will include the results and analysis and Chapter 5 will provide the conclusions of the research and acquired data. Chapter 6 will discuss the recommended future direction of the test and program.

1.3 Statement of Purpose

The purpose of this vibration test is to determine the g-level that the glass reflector will fail in the current mounting scheme, to provide data by which to correlate the analytical models, to develop a baseline by which to compare other mounting schemes, and to test in a cost effective manner.

CHAPTER 2

BACKGROUND

2.1 Mission Overview

The National Academy of Science Decadal Study: "Astronomy and Astrophysics in the New Millennium" (2001) states that the Constellation X telescope will detect hot intergalactic medium and trace other elements heavier than hydrogen and helium over cosmic time [1]. The telescope system will also provide detailed pictures of black holes and sense x-rays across a very large spectrum. In addition to black holes, Constellation X will detect x-rays emitted from the hot gases that collect near dark matter. Dark matter may be a burnt out star or a non-illuminated planet. Other celestial events that are associated with x-rays, such as supernovas will also be visible. Constellation X is a constellation of four telescopes that will be positioned at L2 (a point of gravitational stability 1.5 million km from the earth) and stare into deep space. Figure 2.1 shows the mission profile of the launch and position of the constellation.

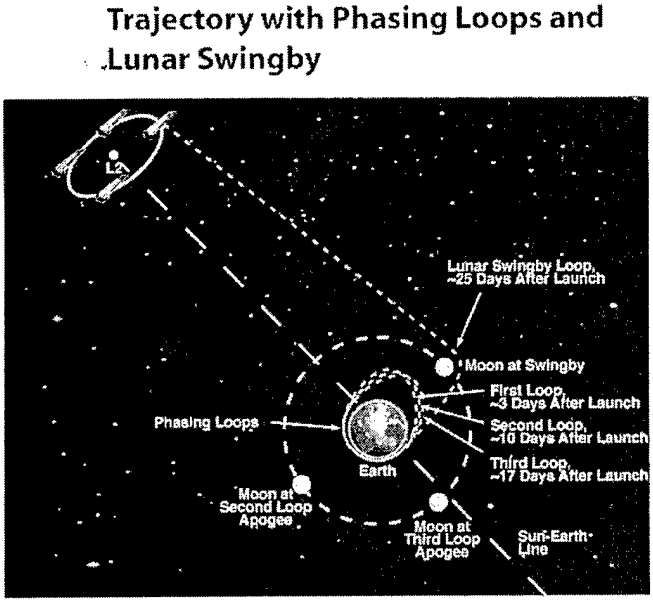

FIGURE 2.1: Mission profile of Constellation X [1].

The mission will consist of launching two satellites simultaneously in the payload compartment of the Lockheed Martin Atlas V or Boeing Delta IV Heavy launch vehicle. After the first two telescopes are launched, the remaining two will be delivered to space in the subsequent months with one follow-up launch. After completing three phasing loops about the earth, a transfer to the moon, a lunar swing-by, transfer, and deceleration to L2, the satellite's onboard hydrazine propulsion system will perform station-keeping operations.

Constellation X is set apart from its competitors and previous missions by the vast amount of effective area present on the spacecraft coupled with the ability to accurately sense x-rays across a large spectrum. The large effective area is a direct function of the number of x-ray reflecting mirrors aligned and mounted in the telescope. There are 16,000 mirrors total in the entire system (4,000 per each individual satellite). The Spectroscopy X-ray Telescope (SXT) will sense energy levels between 0.25 and 10 keV and the Hard X-ray Telescope (HXT) portion will detect the bandpass of 6 keV to 40 keV [1]. Figure 2.2 is a comparison of the effective area of Constellation X as a function of energy for previous missions.

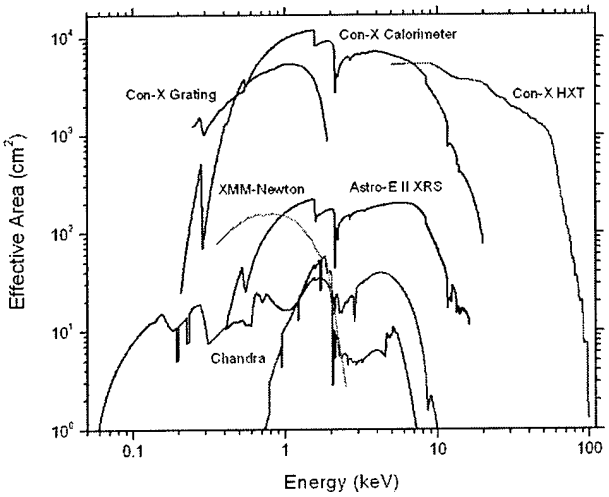

FIGURE 2.2: Energy as a function of effective area [2].

A detailed diagram of one of the telescopes is shown in Figure 2.3. Notice how the satellites will be configured in the payload compartment of the Atlas V or Delta IV Heavy rocket. The mirror substrates, which are the foundation of the research presented in this thesis, are housed in the SXT portion of the observatory.

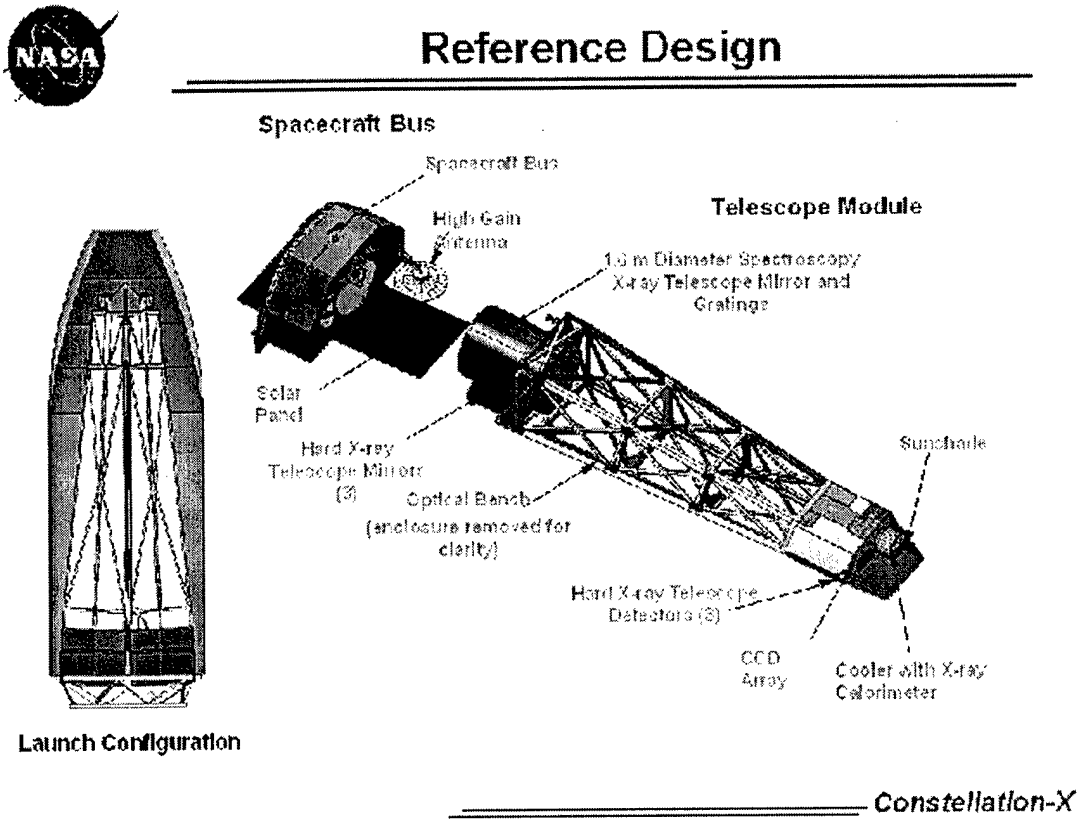

FIGURE 2.3: Reference design of Constellation X [3].

Figure 2.4 is a detailed picture of the HXT, SXT, and Grating Array portion of the observatory. The mirror reflectors are housed in the primary and secondary mirror submodule regions of the diagram. The primary mirror submodule contains parabolic shaped mirrors, while the secondary mirror submodule holds the hyperbolic formed reflectors. An even more in-depth diagram is presented within the following pages.

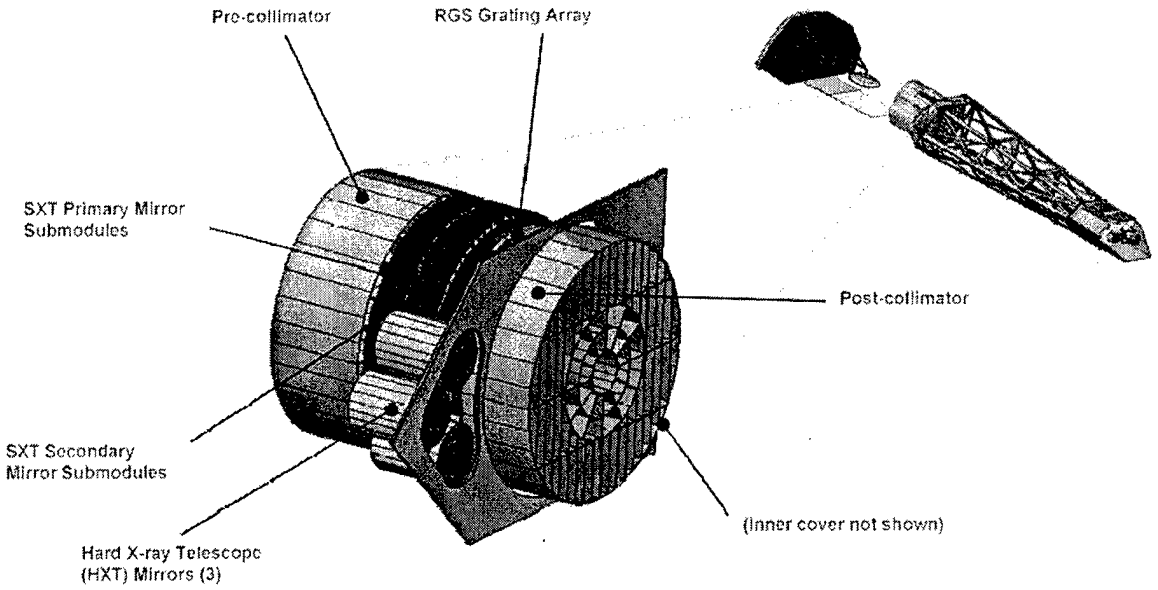

FIGURE 2.4: Diagram of HXT, SXT, and grating array [4].

The primary theory of X-Ray reflection through the SXT portion of the telescope is based on the reflection of X-Rays via a grazing incidence angle created by parabolic and hyperbolic reflectors. This Wolter x-ray concept is shown in Figure 2.5 below.

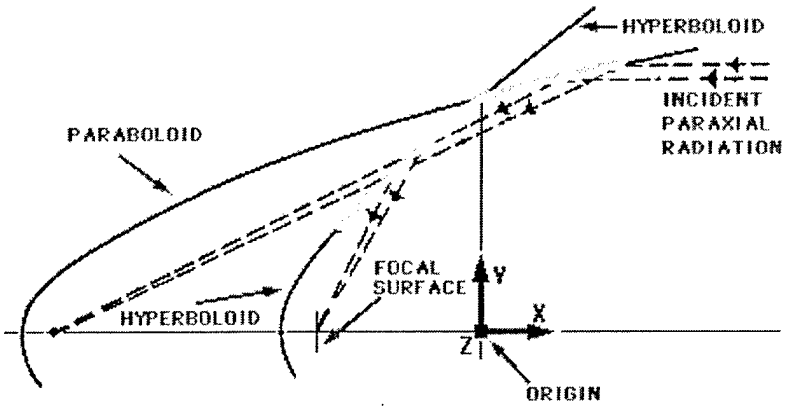

FIGURE 2.5: Diagram of Wolter x-ray concept [5].

Figure 2.6 shows the X-rays being reflected through the SXT. Notice that some X-rays are reflected to the Reflection Grating Spectrometer (RGS) Focal Plane Camera (RFC), while others are concentrated at the X-ray Microcalorimeter Spectrometer (XMS).

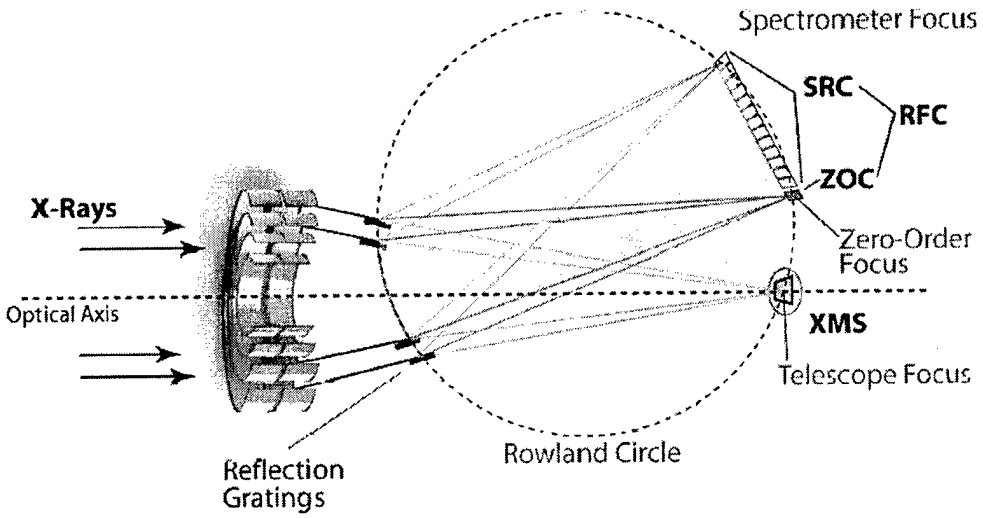

FIGURE 2.6: Reflection and detection of x-rays [4].

The Reflection Grating Spectrometer (RGS) looks at the bandwidth of 0.25 to 0.5 keV. The refection gratings deflect a portion of the X-Rays from the calorimeter array to the quantum calorimeter instead of the Charge Coupled Device (CCD). The calorimeter incorporates thermal and light blocking filters that result in a loss of response. On the other hand, the X-Ray Microcalorimeter Spectrometer (XMS) studies the bandwidth of 0.5 to 10 keV [1].

Figure 2.7 shows the SXT parabolic and hyperbolic mirrors completely mounted in the primary and secondary submodules, respectively. There are approximately 4000 mirror substrates mounted within the P and H modules. The entire module consists of a skeletal housing where wedges of pre-assembled submodules are mounted and aligned.

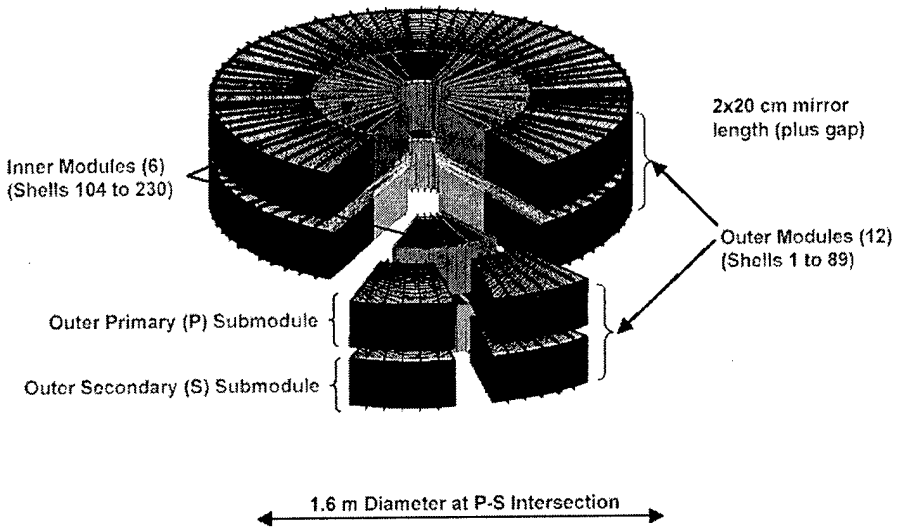

FIGURE 2.7: Diagram of SXT [4].

Figure 2.8 shows a detailed picture of the mounting fixture (part of the SXT) for the mirror substrates. Note that in the current design the glass is held at 5 points, top and bottom, by titanium struts. It will be apparent as the FEM results are explained that the greatest points of stress are at the side edges; therefore proper placement of the struts is important as they introduce point loads on the mirror. Also, the edges of a piece of glass tend to be the weakest as more defects may be introduced through handling and processing.

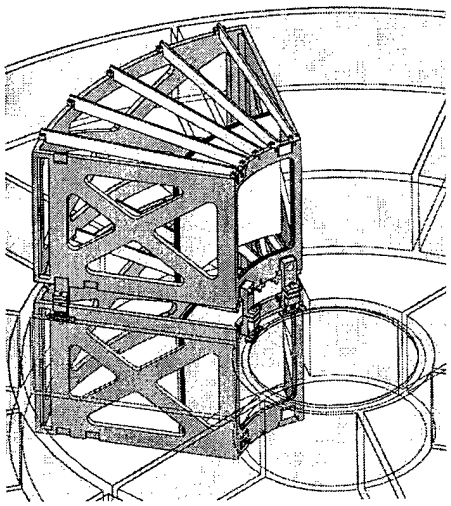

FIGURE 2.8: Wedge fixtures within the SXT [6].

The vibration housing, which is discussed in detail in the Problem Statement portion of this thesis, is designed and built in a manner that attempts to capture the same boundary conditions that the glass will experience in the mounting scheme shown in Figure 2.8.

2.2 Manufacturing of Glass Substrates

It is important to understand the steps of formation and replication of the mirror substrates, as this will make problematic areas more apparent. Dr. William Zhang is devoting a large amount of time to the refining of the glass manufacturing process. Each piece of glass is slumped using a forming mandrel made of fused quartz. After the glass is formed, it is cut with a hot wire to the desired dimensions. Gold is then vapor deposited onto the precise nickel (or Zerodur) mandrel and the glass substrate is coated with a thin layer of epoxy. The glass is then placed on the replication mandrel and the epoxy cures under vacuum to avoid air pockets. The glass then lifts the gold deposit off of the mandrel [7]. Figure 2.9 consists of pictures that show the replication portion of the process. Both the replication and formation processes take place in clean tents.

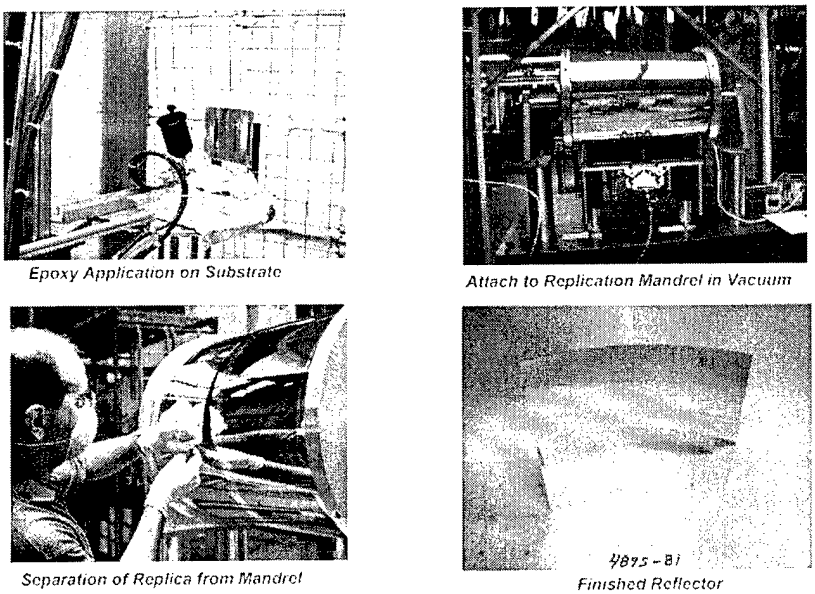

FIGURE 2.9 Dr. Zhang's replication process [4].

Dr. Zhang has become the leading expert in the development of the mirror substrates and is currently focusing on reducing the amount of epoxy used to correct figure distortions and bond the gold to the D-263 glass surface. Dr. Zhang is primarily concerned with obtaining a pristine optical surface within tolerances of 5 Angstroms RMS. Now that he is close in meeting these requirements, much of the program focus has shifted on the survivability and mounting of glass mirror substrates.

Three specific tests were completed on the mirror substrates to determine an accurate understanding of strength and a fourth is currently being conducted. An understanding of this material property is extremely important because it is needed for finite element models. These models predict the forces and survivability of the glass in the launch environment. The results of the 1999 strength test, 2003 strength tests, 2004 strength tests, and current finite element analysis results are discussed in the Background section of this thesis. The results will make it clear that further dynamic testing is warranted and that a comprehensive understanding of the material's properties and behavior are required to determine the survivability.

2.3 Properties of Glass

In order to fully appreciate the results obtained from previous tests of glass strength, there must be a fundamental understanding of the mechanical properties of glass. The strength of glass is determined by the number and types of defects associated with its surface. Narottam P. Bansal and R. H. Doremus of the Materials Engineering Department of Rensselear Polytechnic Institute and the Co-authors of *Handbook of Glass Properties*, state "tiny flaws (cracks) in the surface lead to weakening and failure by brittle fracture. Glass also becomes weaker with time under stress (fatigue)" [8]. Bansal states strength is not an intrinsic property of glass and therefore a table of strengths would not prove useful for analysis [8]. This is primarily due to the

fact that the strength is highly dependent upon the treatment and manufacturing process, handling of the surface, and the relative humidity in the testing environment [8]. Composition has minimal impact on fracture strength however it does significantly influence fatigue [8]. Bansal makes the point that failure stresses of a number of glass samples can vary by a factor of two, even when sample preparation and loading are identical between tests [8]. This random spread of data can make it very difficult to model the strength of the glass. The Weibull distribution used in the last strength test of the D-263 glass is a popular method of modeling the strength of glass [8].

Weibull statistics are commonly used to analyze strength data in ceramic materials [9]. Dr. Arun Varshneya of Alfred University and author of *Fundamentals of Inorganic Glasses* presents the Weibull equation in a form that is easily correlated to ceramic strength test results. The equations for cumulative probability of failure (P) are seen in equation set 2, below [10].

$$P = 1 - \exp[-R]$$
$$R = \int_V [(\sigma - \sigma_u)/\sigma_O]^m dV \quad (for\ \sigma > \sigma_u) \qquad (2)$$
$$R = 0 \qquad (for\ \sigma < \sigma_u)$$

P is the cumulative probability of failure, R is the risk of rupture, σ is the stress over a given volume, σ_u is the minimum stress level for expectation of failure, and σ_O is the normalizing stress parameter [10]. The Weibull modulus (m) and the normalizing stress parameter are normally calculated with statistics software. A simplified version of the cumulative probability of failure (P) and its derivative, the probability density (p) are shown in equations 3 and 4, below [10].

$$P = 1 - \exp\left\{-[\sigma/\sigma_O]^m\right\} \qquad (3)$$

$$p = dP/d\sigma = [m/\sigma_O][\sigma/\sigma_O]^{m-1} \exp\left[-(\sigma/\sigma_O)^m\right] \qquad (4)$$

As previously stated, the surface conditions play a key role in the strength of the glass. Glass substrates that are near pristine or defect free will be stronger than those with surface defects [8]. Temperature also has a large influence on the fracture point of glass. Through experimentation, it can be concluded as a general rule that lower temperatures result in higher fracture strengths [8].

Bansal claims that the fatigue of a ceramic material is dependant upon ambient humidity, material composition, the abrasion, thermal, and atmospheric history of the glass surface, and the applied stress [8]. Modeling the life of a glass sample may be difficult. Fatigue on glass is also determined by the accumulation of time of various stress levels applied to the glass sample. For this reason, the team will initially avoid conducting a random vibration test prior to the sine burst test, as it may be difficult to determine where and when defects were introduced into the reflector.

2.4 Schott Published Data on D-263

The published data on the D-263 in untreated un-slumped form is seen in Table 2.1 below. A ceramic (brittle) material was necessary to minimize deformation, which may be less controllable with a ductile material. Also, D-263 has excellent optical and surface qualities, is manufactured in thin sheets, and has a reasonable coefficient of thermal expansion (CTE). The annealing and softening points are temperatures that are easily reached in commercial ovens.

TABLE 2.1: Schott published D-263 properties [11].

Thermal Properties			
Viscosity and Corresponding Temperatures			
Designation	g η [dPas]	Temperature θ [°C]	
Strain Point	14.5	529	
Annealing Point	13	557	
Softening Point	7.6	736	
Transformation Temperature Tg in °C		557	
Coefficient of Thermal Expansion α			
Coefficient of Mean Linear Thermal Expansion α(20-300°C) in 10 -6 K -1 (Static Measurement)			7.2
Mechanical Properties			
Density ρ in g/cm3 (annealed at 40°C/h)			2.51
Stress Optical Coefficient C in 1.02 · 10-12 m2/N			3.4
Young's Modulus E in kN/mm2			72.9
Poisson's Ratio μ			0.208
Torsion Modulus G in kN/mm2			30.1
Knoop Hardness HK100			590

Focusing on the mechanical properties, it is shown in the 1999 strength tests that the glass loses a significant amount of strength after being handled and subjected to Dr. Zhang's slumping process.

2.5 Results of 1999 Strength Test

The 1999 strength test performed by Dr. Charles He was a ring-on-ring biaxial test, which used flat specimens and test setup as shown in Figure 2.10. This particular test also evaluated AF45 and Silicon wafers in addition to the D-263 [12]. The samples were evaluated at thicknesses ranging from 0.3-1.1 mm [12]. An additional set of D263 0.4mm samples were heated to evaluate the effects on strength introduced by slumping the glass [12].

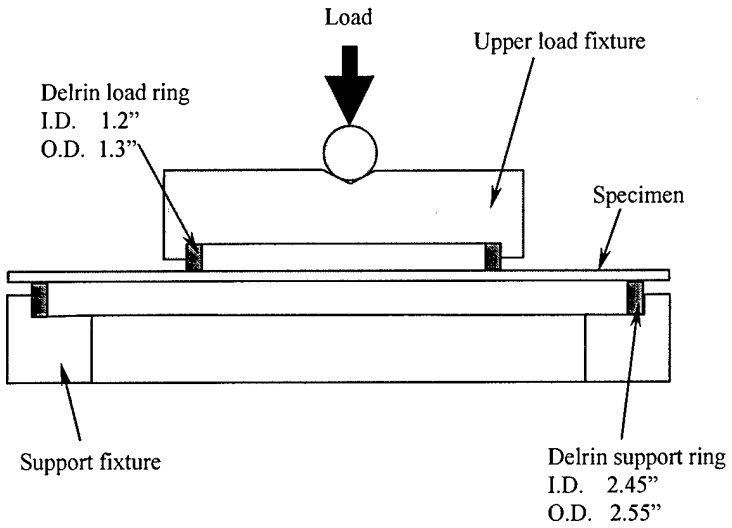

FIGURE 2.10: Ring-on-ring biaxial strength test [12].

Previous studies have shown that the ring-on-ring biaxial strength test does not account for edge effects. In many cases the edges in a ceramic material contain the majority of defects, which account for the weakening of the material. Figure 2.11 displays the 1999 biaxial test strength data.

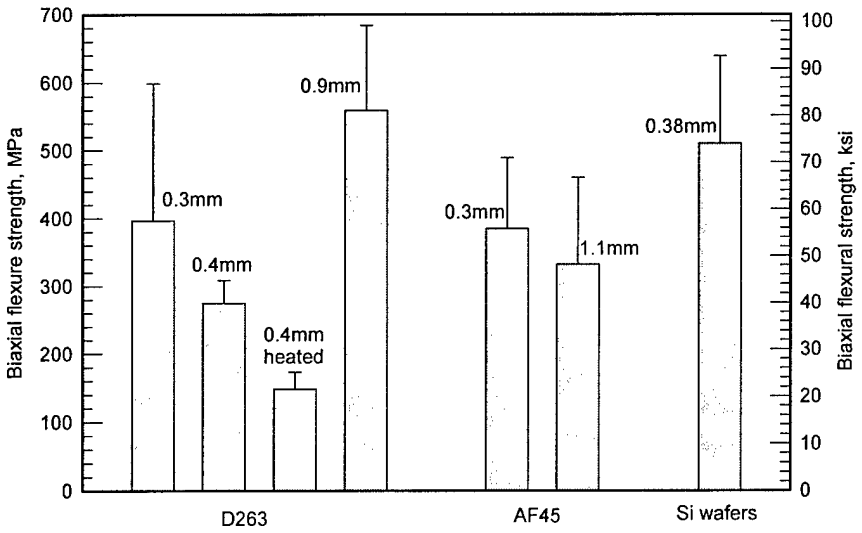

FIGURE 2.11: Biaxial strength data [12].

This chart shows that the heated D-263 glass looses nearly half of its original strength. This reduction of strength may be detrimental to mission survival, which is evaluated through the dynamic test on the shaker table.

2.6 Results of 2003 Strength Test

In order to more completely understand the strength of a slumped piece of D-263, Dr. Charles He recommended that the researchers conduct a bend test of the glass. Andrew Carlson, Dave Puckett, and Dr. Len Wang played important roles in the testing. The bend test accounts for the edge effects, so a decrease in strength from the ring-on-ring biaxial test was expected. The greatest stress is present in the center of the sample in a region perpendicular to the applied load. The majority of samples initiated fracture close to this central region. If the glass mirrors were manufactured perfectly then there would be one fracture in the center of the glass (assuming symmetric test sample) horizontal to the floor (perpendicular to the applied loads), however this was not the case. Some of the fracture patterns branched out from their fracture origin. The bend test looked at three different samples as seen in Figure 2.12 below. The samples are gold/epoxy coated, silver coated, and clear.

FIGURE 2.12: Pictures of test samples.

The test itself compressed the glass perpendicular to its weakest axis using an Instron 4442 Machine shown in Figure 2.13.

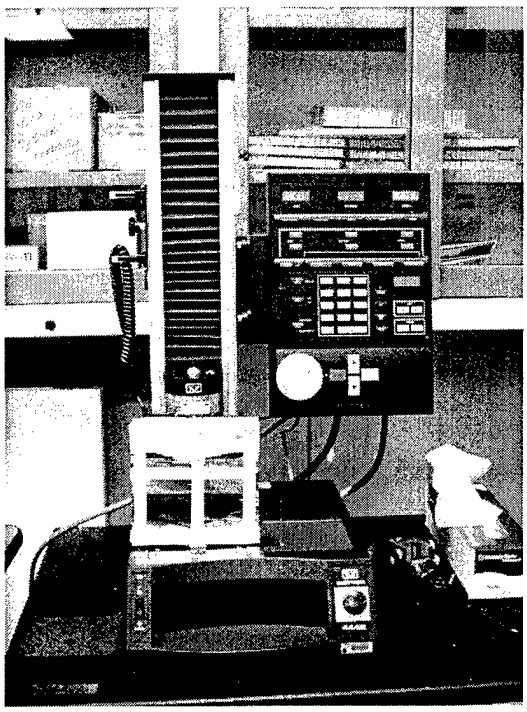

FIGURE 2.13: Picture of Instron machine and test setup.

After Dr. Charles He, Andrew Carlson, and Dave Puckett completed the test, Dr. Charles He and Andrew Carlson photographed and sketched the fracture patterns. Dr. He took the analysis a step further and examined the fracture origins under a microscope to determine their cause as seen in Figure 2.14.

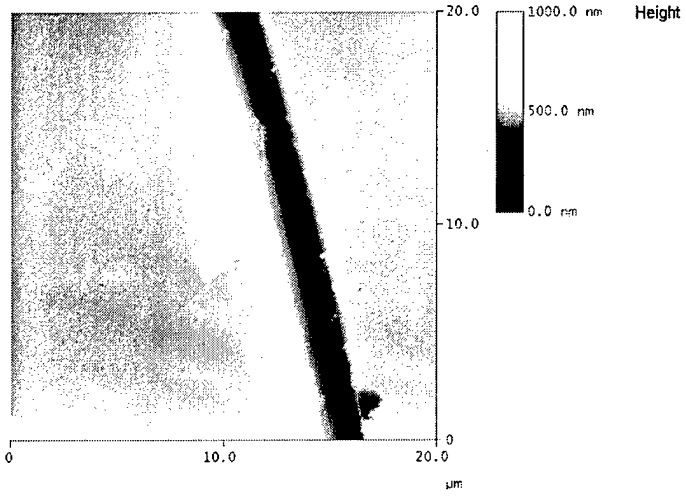

FIGURE 2.14: Atomic Force Microscopy (AFM) showing groove that caused failure in sample 489S-80 [12].

Roughly half of the fracture origins were at the surface, which was unexpected to the researchers and scientists as the edges tend to contain the most defects.

Figure 2.15 shows the strength results from the test. With the exception of the silver coated mirror samples, the strength of the other samples was similar. Dr. He stated that the results of the 2003 test painted an accurate picture of the strength of the glass despite the fact that there were not a statistically significant number (30) of samples. A Weibull distribution was used to establish the uncertainty bars on this particular chart.

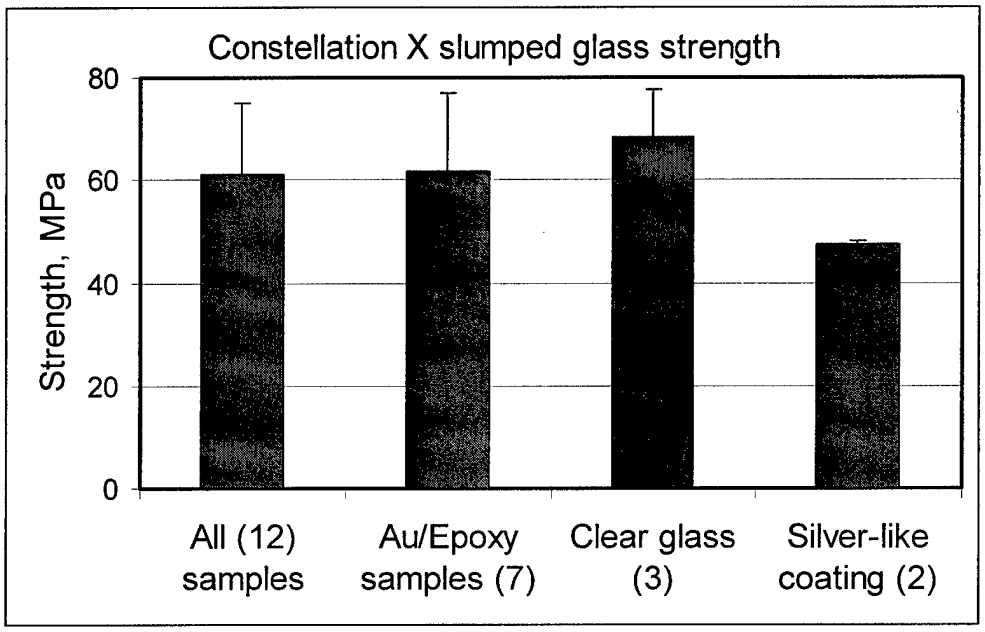

FIGURE 2.15: Overall results of the 2003 study [12].

Figure 2.16 compares the 2003 strength tests with the 1999 strength tests. The larger decrease in strength of the 2003 results was due primarily to the differing test setup and accounting for the edge effects. Notice also the 50% reduction in strength of the 1999 results when the glass is subjected to the slumping process.

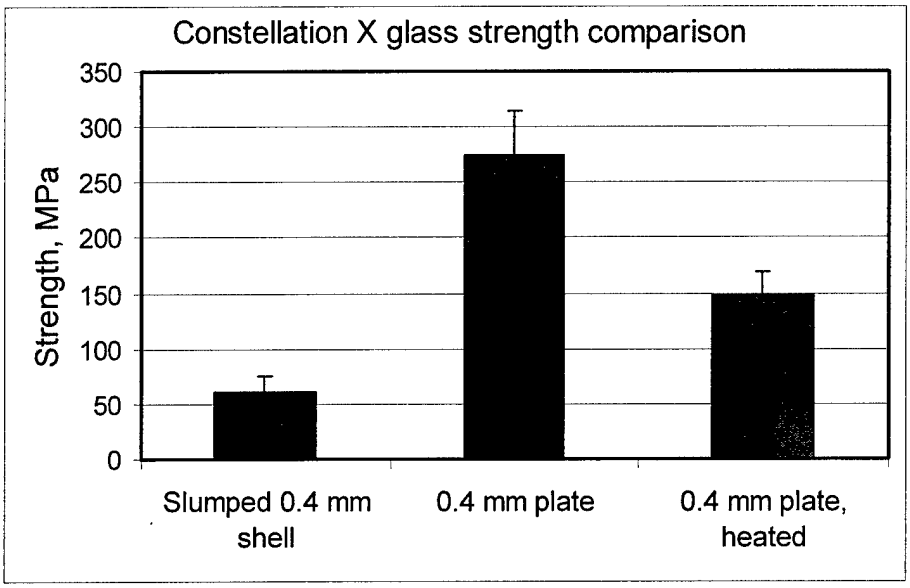

FIGURE 2.16: Comparison of data to previous (1999) study [12].

From this study it is apparent that the average strength of the glass is around 8.5 ksi. This is half of the strength that was previously being incorporated into the finite element models portraying the application of launch vehicle forces.

2.7 2004 Strength Tests

It was explained that handling of glass may result in additional defects and therefore a reduction in strength or an increase in data scatter. Also, if the vendor and distributor do not utilize consistent handling procedures, the strength properties between different orders may vary. This study is important as it may help to explain phenomena associated with failure levels and fracture origins caused by the vibration test.

Charles He, Len Wang, Paul Reid of Harvard-Smithsonian Center for Astrophysics, and Walter Thomas of NASA-GSFC launched a glass strength study with two distinct objectives. These objectives were to determine the lot variation in the strength of as-received glass plates and the effects of cleaning on the strength of glass plates [13].

The test procedures were similar to those discussed in the 1999 glass strength test. It consisted of a ring-on-ring strength test setup. There are no edge effects considered unlike the bend strength test which occurred in 2003. Ring-on-ring strength tests only account for surface defects. A geometric non-linear elastic model was used with the finite element analysis since the deflection was much larger than the thickness of the glass [13]. The thickness for the test specimens was 0.4 mm. The dimensions of the Schott D263 borosilicate glass were 100 x 100 x 0.4 mm [13]. The test used to determine the lot variation of glass received consisted of 4 different glass plates from different deliveries [13]. Each glass plate was diamond cut into about 20 samples. The test used to determine the effects of cleaning on the glass plates used 5 cleaned glass plates, which were cut into about 15 specimens [13].

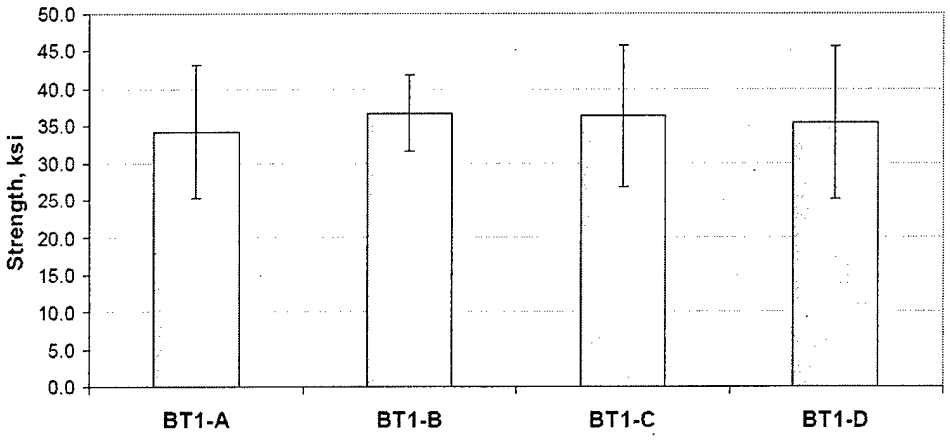

FIGURE 2.17: Glass strength as received for four batches [13].

The test determining the strength variation among deliveries concluded that there was no statistically significant difference in the average strength between the four deliveries as seen in Figure 2.17. The samples from one of the deliveries however, did have a higher Weibull modulus, which means that there was lower strength scatter [13].

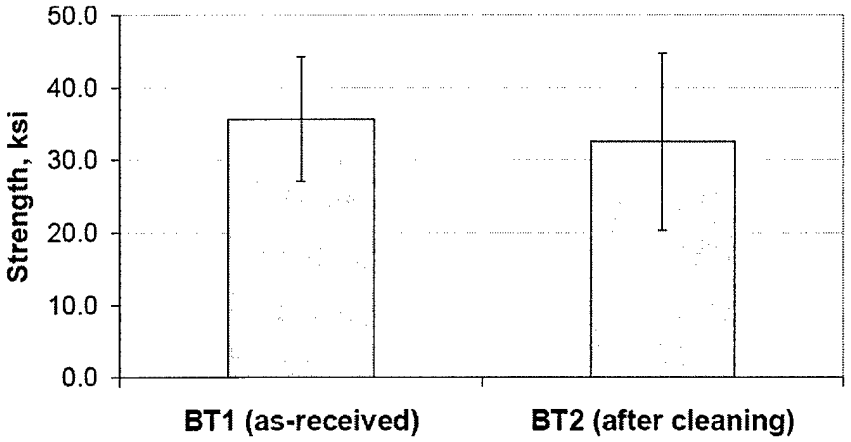

FIGURE 2.18: Reduction of strength caused by cleaning [13].

The test determining the effect on strength by cleaning the samples concluded that cleaning decreased the average strength by 9% and the Weibull modulus by 37% [13] as seen in Figure 2.18. There was a 50% reduction in stress at a 1% probability of failure [13].

2.8 FEM Dynamic Modeling Results

Janet Squires has completed an in-depth analysis of the expected forces of the launch vehicle on the Constellation X satellite (using GEVS method). It should be noted that the GEVS method is a relatively conservative modeling standard. The results show that the glass will not withstand the introduced loads of launch.

Below is a chart explaining the Factors of Safety (FS) required by NASA for the use of various materials. Note that the FS for glass is 3.0 with qualification through test. This is primarily due to the unpredictability and large scatter in strength data.

TABLE 2.2: Factor of safety requirements [6].

Structure	Qualified by Test		Qualification * Test Factor	Acceptance or Proof * Test Factor	Qualified by Analysis Only	
	Yield	Ultimate			Yield	Ultimate
Metallic	1.25	1.4		1.2	2.0	2.6
Fastener and Preloaded Joints	1.2 (Joint Separation)	1.4		1.2		
Composites & Bonded Joints		1.5		1.2		
Glass (Nonpressurized)		3.0		1.2		5.0
Glass Bonds		2.0	1.4	1.2		

*Note: Qualification Tests are performed on flight-like hardware, while Acceptance or Proof Tests are performed on actual flight hardware.

Below is an Excel spreadsheet tool developed by Janet Squires, which calculates the Margin of Safety (MS). As seen in Table 2.3, this tool presents a negative MS of -0.99 for the use of D-263 in the current fixture, which is unacceptable. The survivability of the glass must be validated and verified through dynamic testing.

TABLE 2.3: Spreadsheet tool outputs [6].

SXT Mirror Stress

Fill in yellow boxes.

A	Stress due to Launch Load (ksi)	25.6	
B	Stress due to Preloading Glass (ksi)	0.9	Note: May not want to apply factor of safety to preload stress
C	Stress due to Thermal Load (ksi)	0.0	
D =A+B+C	**Total Glass Stress (ksi)**	**26.5**	
E	Glass Factor of Safety	3.0	Design must be qualified by Test
F	Temperature Degredation Factor	1.0	
G	Stress Concentration Factor due to microcracks	1.0	
H	Factor due to epoxy/gold layer	1.0	
I = E*F*G*H	**Total Stress Factor**	**3.0**	
J	**Glass Allowable (ksi)**	**1.0**	0.4 mm slumped glass
(J/(I*D)) -1	**Margin of Safety**	**-0.99**	

Figure 2.19 is a diagram showing the stress distribution on the face of the glass when a 1 g load is applied radially inward. This model simulates the mirror being attached to struts at 5 points on the top and bottom. It makes sense that this sort of fixture could introduce point loads that are detrimental to the survivability of the mirrors when undergoing launch.

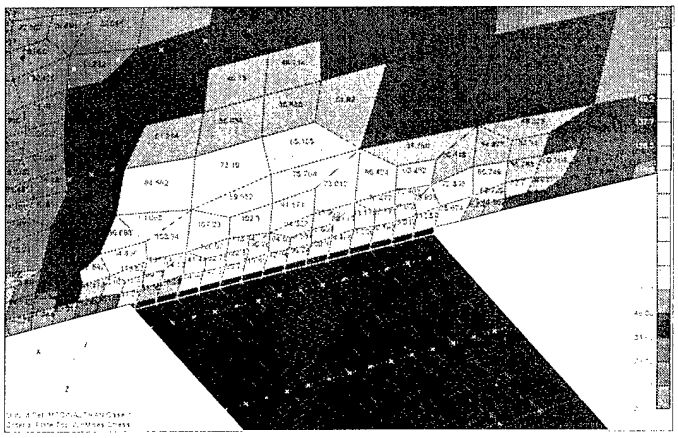

FIGURE 2.19: SXT mirror with 1 G applied radial inward [19].

Notice that the highest stress levels appear on the edges and in the upper right corner with respect to the glass oriented as shown. This is not a great compliment to the results of the 2003 strength test, which show the edges as highly likely to fracture. This finding will drive the placement of struts in the design, but other factors such as effective area, natural frequency, and deformation are constraining. A vibration test is needed to determine what will actually happen to the D-263 when subjected to dynamic loading.

2.9 Vibration Testing Techniques with a Shaker table

It is important to understand that actual data for the Atlas V launch vehicle is not readily available, which results in conservative numerical calculations of expected forces in the finite element models. Also, consideration is still being given to using the Delta IV heavy. The NASA specification used by Janet Squires in her FEM is the GEVS method of estimation. A launch vehicle generates three major dynamic conditions [14]. The first condition is high frequency acoustic loads caused by engine-generated noise during ignition and liftoff [14]. It is also caused by the variation in pressures during launch and reentry [14]. The second condition is random vibration loads induced by engine-generated excitations both acoustically and through the structure [14]. The last major condition is the low frequency structural loads, also created during liftoff and landing [14]. The combination of these loads may be represented in Equation 2 shown below, where N_i is the combined load factor, S_i is the steady-state load factor, L_i is the low-frequency dynamic load factor, and R_i is the high-frequency random vibration load factor [15].

$$N_i = S_i \pm \left[(L_i)^2 + (R_i)^2 \right]^{1/2} \qquad (2)$$

NASA's document, *General Environmental Verification Specification (GEVS) for STS and ELV Payloads, Subsystems, and Components, Revision A*, provides strict guidance to

completing a satisfactory vibration test that will accurately simulate the launch conditions mentioned above.

A sine sweep and a sine burst test are two key areas where the test team will focus their efforts. In order to understand and predict the structural response of a spacecraft or its subsystems, one must establish the excitation and structural characteristics of the system [16]. The modal frequencies are most commonly used to establish the basic properties of the system during dynamic testing [16]. NASA states in their GEVS-SE Revision A document that modal tests should be performed for every payload to validate the accuracy of the analytical model and to make changes accordingly [15]. A low-level sine survey is acceptable for establishing the fundamental frequency of the subsystem [15]. The boundary conditions of the subsystem should accurately reflect those that will be present during flight [15]. Also, the various interfaces of the subsystem and their respective flexibilities must be considered when they do not precisely reflect those that will be present during launch [15]. The natural frequencies obtained from the low level sine sweep will validate the analytical models and allow for the test team to determine if structural damage to the fixture occurred between tests [15]. Other causes for deviations in natural frequencies could be variation in material properties, randomness in structural dimensions, changes in the character of internal joints, and changes in the boundary conditions [16].

NASA's guide states that the design must also be strength tested to 1.25 times its limit loads [15]. NASA poses 5 questions that should be considered when preparing a dynamic test [15].

(1) Which method most closely approximates the flight-imposed load distribution?

(2) Which can be applied with the greatest accuracy?

(3) Which best provide information for design verification and for predicting design capability for future payload or launch vehicle modifications?

(4) Which poses the least risk to the hardware in terms of handling and test equipment?

(5) Which best stays within cost, time, and facility limitations?

NASA also explains that the subsystem should be mounted to the mechanical interface with a setup that is the same as actual conditions [15]. The functionality of the equipment, both hardware and software, will be checked and consistently monitored throughout the testing process [15].

It is accurate to say that ceramic materials of this shape and size have never before been dynamically tested in a fixture exactly like the one designed by the Mechanical Systems Engineering Team. Therefore the data obtained will be unique to the test team's particular experiment and the numerical results of previous dynamic ceramic tests are not completely applicable. What previous studies do show are acceptable methods of testing to include general expectations such as a large scatter in data and the need to use statistical models such as Wiebull analysis. Previous vibration tests also provide insight and explain problems that may occur when interpreting the data. An in-depth analysis was launched into previous dynamic tests conducted. The findings of this research are presented below and the lessons learned are applied to the dynamic testing performed by Andrew Carlson on the shaker table.

The AIAA paper, *Structural Evaluations and Dynamic Testing of Solar Electric Propulsion Components*, by J.R. Womack and Jay-Chung Chen most closely resembled the shaker table provided to the Constellation X Mechanical Engineering Team at NASA Goddard. After reviewing this journal, it was apparent that despite minor differences in dynamic testing of a structure, 3 main stages should take place if resources are available. The first stage is low

frequency modal tests, the next stage is high frequency modal tests, and the last stage is forced vibration tests.

In order to complete the low frequency modal tests, an oscillator-amplifier unit, a mechanical shaker, two accelerometers, an oscilloscope, and a teletype are warranted [17]. The unit to be tested is placed on the shaker. One accelerometer is positioned adjacent to the shaker attachment point to act as a reference for the other accelerometer, which will act as a rover [17]. The space part is then vibrated using an oscillating force generated by the shaker and controlled by the power amplifier and oscillator [17]. The input force was less than one gn and the frequency of the shaker was altered until a resonant condition was produced [17]. A resonant condition means that the external excitation frequency of the shaker is equal to that natural frequency of the spacecraft part being tested [17]. Resonance is apparent when there is a peak response of the voltage output of the reference accelerometer [17]. At this point the rover accelerometer measured various points on the spacecraft part. The key is to start at the lowest frequency generated by the oscillator and increasing through a range of frequencies until the resonant frequencies and various portions of the spacecraft are determined [17]. Low frequencies are considered the range from 0 to 150 Hz.

High frequency modal testing presented in the AIAA paper claimed that using the same method would prove entirely inefficient due to the large size of the space part, the need to cover various locations, and varying the frequencies from 150-2000 Hz [17]. This particular test used vibration holograms, which represent various vibration patterns generated at a high frequency. The structure discussed in the AIAA 72-442 paper is much more complex and larger in size than the OAP 2 housing that will be used as a fixture for the mirror substrates.

The last test is the forced vibration test. First an "integrity sweep" at 0.5 Grms from 10-2000 Hz was conducted to determine amplification factors so that the range of responses to be detected by the accelerometers could be initially estimated [17]. After the integrity sweep, the accelerometers were adjusted so that the optimum range of data during the first sweep would be recorded [17].

Another dynamic technique that is applicable to our particular dynamic test is known as sine burst testing. Donald A. Barnes and James T. Pontius discuss this technique thoroughly in their paper, *Structural Qualification of a Spacecraft Payload Using Near-Resonance Sine Burst Testing*. In general, the driving frequency of the shaker will be much less than the first resonant mode of the structure being tested, allowing for uniform acceleration [18]. The experimental approach to this type of analysis is to perform a low-level random vibration test similar to that previously explained to verify and possibly alter the analytical sine burst test parameters [18]. Then a reduced-level sine burst test should be accomplished to test for linearity and to validate the parameters previously dictated [18]. Third, run a qualification-level sine burst test, which is where the primary data will be generated [18]. Lastly re-run the low-level random vibration test and compare the results to the initial [18].

A low-level vibration test will expose the dynamics of the tested spacecraft part on the shaker table [18]. The transfer functions that are generated during this initial test will display the primary modes and the level of dynamic amplification that is present in each particular mode [18]. At this point the acceleration ratio may be calculated by comparing the actual acceleration at two points previously dictated [18].

The reduced level sine burst test should be conducted at 10% of Test Limit Loads (TLL) to verify initial test parameters. This is accomplished by comparing actual loads to those

previously calculated through analytical methods [18]. The acceleration ratio also needs to be calculated and the test parameters adjusted so that the correct acceleration ratio is reached and linearity is present in the results [18].

Lastly, the input acceleration should be increased to 80% TLL in 20% increments [18]. Once 80% TLL is achieved, the increments should decrease to somewhere between 5-10% [18]. At each level, the results should be checked for linearity, a constant acceleration ratio, and the internal loads should be compared to analytically derived values [18].

After a study into previous dynamic tests using shaker tables, a few themes seemed apparent. First, a sine sweep should be run as an initial test to determine the natural frequencies in each axis. Secondly, a sine burst test should be conducted to simulate and test the high g forces expected on launch. Third, a post test sine sweep should determine the structural integrity of the test article after shock. These three steps will be the heart of the test team's dynamic test procedures, which are presented in the following section, the Problem Statement.

CHAPTER 3

PROBLEM STATEMENT

3.1 Purpose of the Test

This test has four distinct objectives that define the purpose. The purpose of this test is to understand at what g level the glass will fracture in the current mounting scheme, to provide data by which to correlate the design team's analytical models, to create a baseline by which to compare other mounting schemes, and to develop a low cost vibration test.

In order to meet these challenges, a number of steps must be taken and discussed in order to ensure an accurate simulation of launch loads on the mounted reflector. First, the engineering team designed a fixture, which was then created in IDEAS by Bobby Nanan, the team designer. William Davis then performed thermal analysis on the design to determine the materials that would be needed. Chris Kolos machined the fixture and Andrew Carlson assembled the fixture and bonded a reflector with the help of Bobby Nanan. Janet Squires of Swales provided results from her models that would predict how the glass behaves in a dynamic environment. The failure predictions were studied and used to drive a test plan and procedure. After the analysis, a detailed description of the test setup, test matrix, and test procedures were developed by Andrew Carlson. Jeff Stewart and Andrew Carlson provided oversight of the engineering processes.

3.2 Test Matrix

The test matrix for this test is seen in Table 3.1. The table shows the type of data collection that the test team requires. This thesis will only incorporate one test or one data point. The test team has about 30 samples ready to test, but the division of this set (samples per axis

and/or mounting method) will be determined after the team develops an understanding of the reflector's behavior when subjected to a load in the radial direction.

TABLE 3.1: Test matrix.

Sample	Axis Tested	Modal Information (Hz)	G-Level of Failure (gn, Hz)
Sample identifier Ex: 489 S-88	x, y, or z-directions as defined by the fixture label above	What were the natural frequencies obtained during the sine sweep?	Level where failure occurred for the corresponding sample

The sample set of mirrors contains both the parabolic (primary-P) and hyperbolic (secondary-H) figures. This means that two different strut cutouts in the titanium plates needed to be designed. The sample set contains 14 parabolic reflectors and 21 hyperbolic reflectors as seen in Table 3.2.

TABLE 3.2: Sample set.

Parabolic-Primary-P	Hyperbolic-Secondary-S	
489 P-95	489 S-101	489 S-70
489 P-51	489 S-121	489 S-73
489 P-94	489 S-33	489 S-72
489 P-121	489 S-167	489 S-74
489 P-32	489 S-100	489 S-78
489 P-75	489 S-99	489 S-79
489 P-92	489 S-105	489 S-88
489 P-76	489 S-102	489 S-120
489 P-62	489 S-97	
489 P-88	489 S-94	
489 P-90	489 S-84	
489 P-81	489 S-85	
489 P-80	489 S-92	
489 P-38	489 S-123	

3.3 Design and Assembly of the Vibration Fixture

The vibration testing incorporates a Ling Dynamic Systems (LDS) vertical shaker coupled with a DVC 48 digital vibration controller. Analytical modeling, completed by Janet Squires, has revealed that the critical force is in the radial direction (orthogonal to the mirror

center) and parallel to the z-axis. In other words, this is the most sensitive direction of the reflectors to inputted loads. The design team produced a fixture for the test that would accurately simulate the boundary conditions associated in flight and also allow for testing on all three axes. A picture of the fixture and labeled axes are shown in Figure 3.1 created by Bobby Nanan.

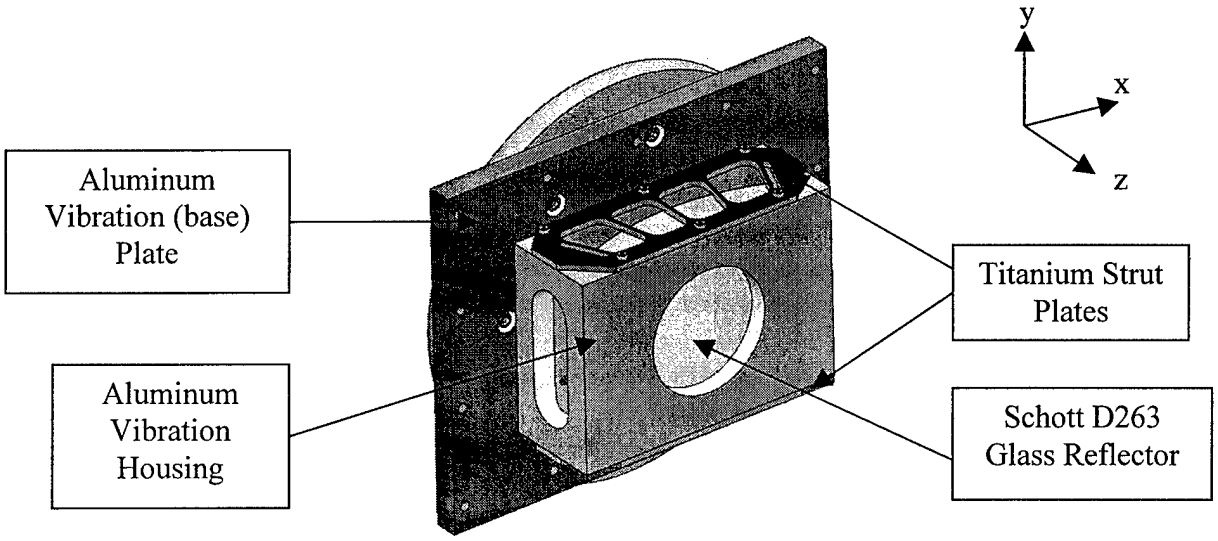

FIGURE 3.1: IDEAS drawing of the vibration fixture by Bobby Nanan (Swale).

The fixture is constructed of an aluminum housing with two titanium strut plates, bolted on the top and bottom of the housing at eight positions. The overall mass of the fixture is 32.945 lbs. The 6061-T651 aluminum vibration plate is 18.89 lbs. The 6061-T651 aluminum housing is 12.25 lbs and the 2 titanium strut plates weigh 1.71 lbs. The reflector weighs 0.095 lbs. The primary reason for using the stated materials was derived from a tradeoff study and discussion on thermal analysis of the vibration fixture.

Thermal Expansion issues were modeled by William Davis and discussed by the NASA Con-X SXT Mechanical Systems Engineering Team. The design team had to determine whether to use aluminum, a relatively cheap material, or titanium, which has a more favorable coefficient

of thermal expansion. The analysis of Bill Davis concluded that 1 deg C delta T would result in an additional 304 psi in glass stress for aluminum and 43.3 psi in glass stress for titanium. Davis also concluded that if the test environment was maintained to within 3 deg C delta T that an additional stress of 800 psi could be introduced into the glass, which could result in about a 5% change in stress if the hypothetical glass strength was 16 ksi. The design team decided that the housings should be made of aluminum in an effort to save time and money, but that the strut plates should be titanium as this is where the critical interface between the glass, epoxy, and strut is present.

In addition to thermal expansion, Andrew Carlson consulted with Eli Ahronovich to determine any vibration issues with the design. Ahronovich explained that there should be no excessive overhang of the base plate as this may create additional noise. Chris Kolos therefore trimmed the corners of the aluminum vibration (base) plate. It was also pointed out that bolts should be no less than 2.5 inches apart; as a general rule, the more bolts or attachment points, the better for ensuring rigid body motion. For the testing of the x and y axes, the center of gravity may be adjusted using counterweights. Ahronovich also suggested adding accelerometer holes on all surfaces (including a few extra holes) to make it convenient to move the accelerometers to various surfaces to identify and isolate vibration problems. He suggested that magnesium is a great vibration plate material because of the damping characteristics, but machining issues, availability, and cost forced the engineering team to proceed with the aluminum vibration plate. The dimensions and design specifics of the vibration housing are seen in Figure 3.2 created by Bobby Nanan.

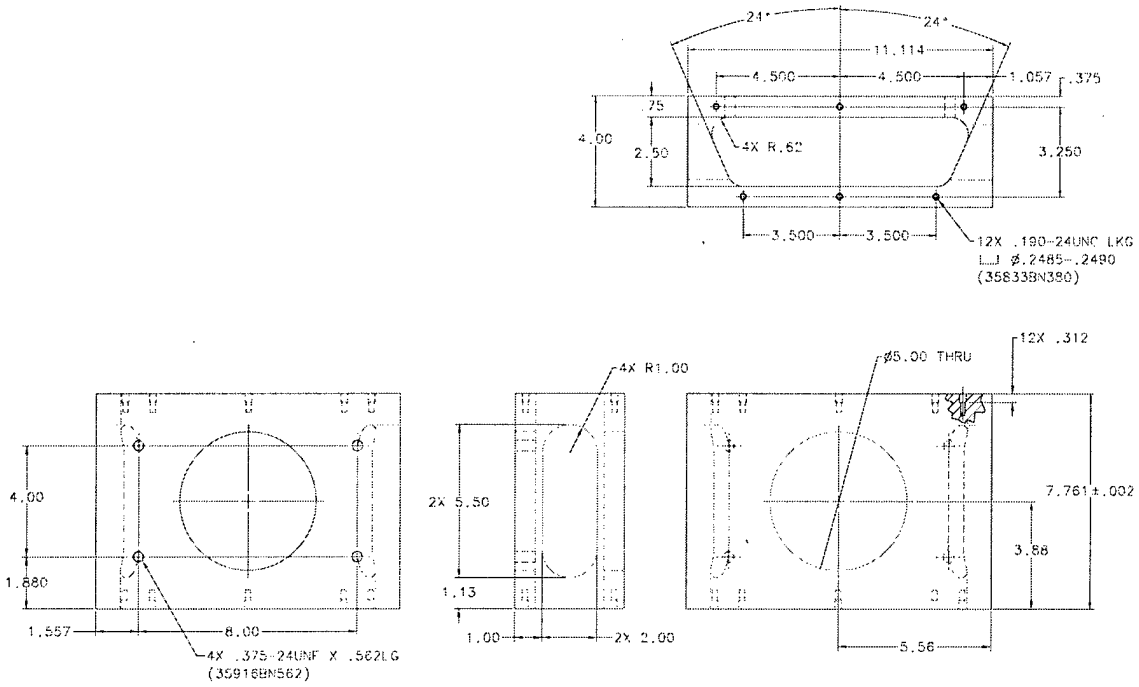

FIGURE 3.2: Dimensions of the vibration fixture by Bobby Nanan (Swale).

After designing and machining the fixture, the aluminum housing and titanium strut plates must be cleaned. This ensures that the epoxy will completely bond to the metal components. At this point, key steps must be followed in the assembly of the vibration fixture to ensure clean bond lines and a stress free reflector. The titanium plate was attached to the vibration housing by securing bolts in an opposite and alternating fashion. Three mil shims were then inserted into the strut grooves to ensure an even bond line. Andrew Carlson then applied EA9394 structural adhesive in the strut groove and set the glass into the grooves, assuring no contact with the titanium. Bobby Nanan ensured that the P end of the reflector was associated with the P strut plate and that the S end of the reflector was associated with the S (or H) plate. The top plate was then attached in the same manner as the other strut plate and epoxy was injected through the bonding ports, ensuring the glass was neither stressed nor contacting the titanium. Figure 3.3 shows a three mil bond line between the reflector and the titanium strut.

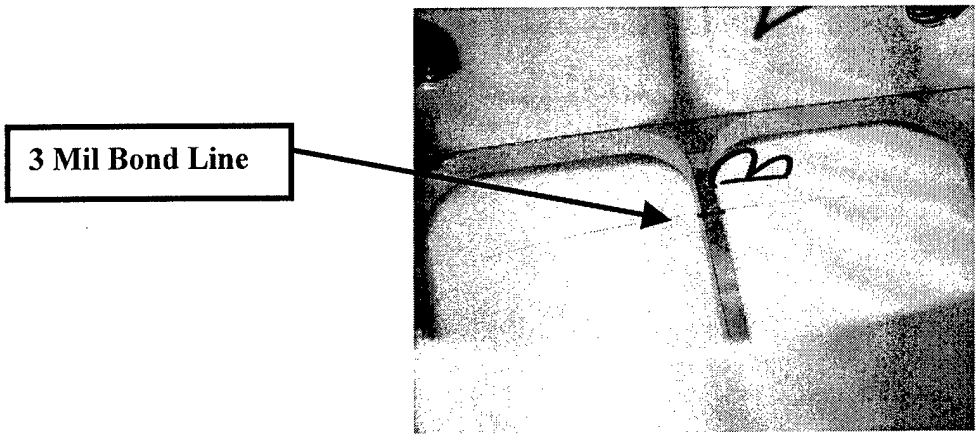

FIGURE 3.3: Close up of 3 mil bond-line attaching the reflector to the titanium strut.

The bolts attaching the titanium strut plate to the aluminum housing were torque striped using ¼ circle lines of epoxy around the bolt head and titanium plate interface. This allowed the team to determine if there was any structural failure in the titanium plate and aluminum housing interface during vibration. When the epoxy set, the bolts holding the bottom titanium plate were torque striped. EA 9394 structural adhesive should cure for at least five days. Figure 3.4 depicts a bonded reflector and also shows the bolts securing the titanium plate to the aluminum housing, which are to be torque striped.

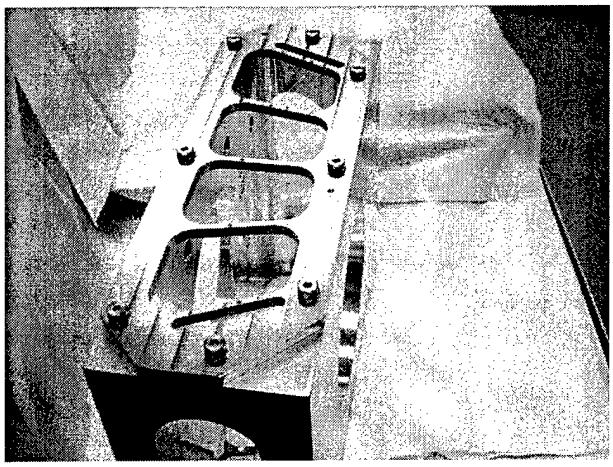

FIGURE 3.4: Reflector bonded in the vibration fixture.

The team has 14 primary substrates and 21 secondary substrates total and therefore machined 4 pairs of titanium strut plates to fit the parabolic mirrors and 6 pairs for the hyperbolic (S) mirrors. The reason that 10 vibration housings were manufactured is that the design team would like to keep the testing process as continuous as possible, with the primary cause for any delay being the required cure time for epoxy bonds.

3.4 Finite Element Analysis and Failure Predictions

Janet Squires completed the FEM on the vibration fixture, reflector, and base plates. Figure 3.5 shows a depiction of the test article created in NASTRAN.

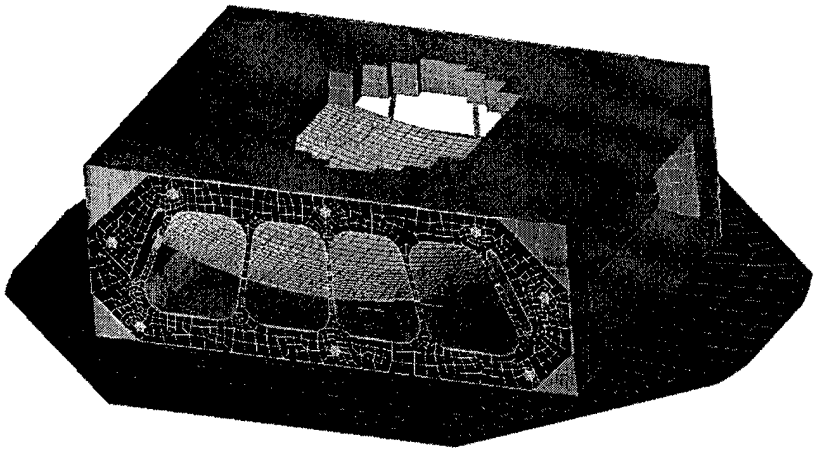

FIGURE 3.5: FEM model of the vibration fixture [19].

The 1st mode of the reflector was determined to be 168 Hz as seen in Figure 3.6. Sine burst testing should take place at a much lower frequency to avoid excitation or departure from a controlled environment. The frequency used in the sine burst test was 25 Hz.

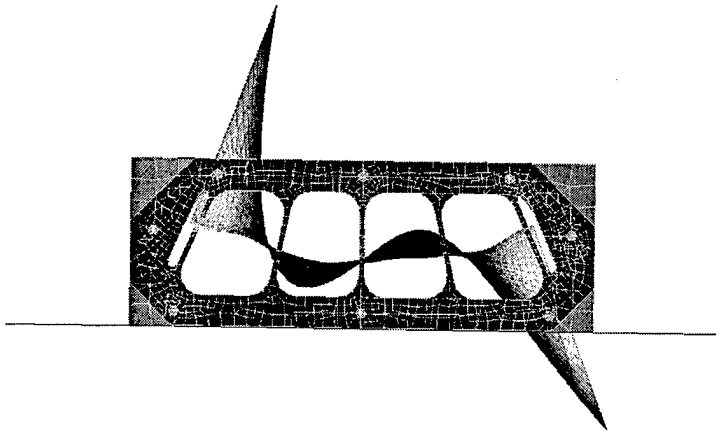

FIGURE 3.6: 1st mode of the vibration fixture [19].

The second mode of vibration was determined to be 175 Hz as seen in Figure 3.7.

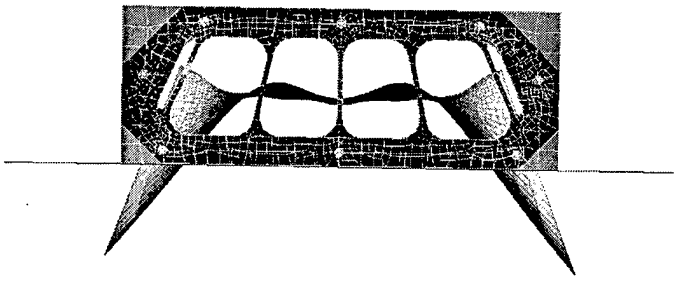

FIGURE 3.7: 2nd mode of the vibration fixture [19].

Janet Squires' analysis predicts that the reflector will fail at 46.2 gn. This assumes a glass strength value of 8.5 ksi. Other assumptions include that no microcracks are present in the reflector [19]. Microcracks will in fact lower the allowable of the glass. The reflector studied is

not the worse case scenario or largest reflector in the telescope system. Future tests on this worse case scenario, caused by the larger spaces between struts, must be accomplished to validate the glass for flight.

3.5 Test Setup

The test consists of a Ling Dynamic Systems (LDS) Force Vibration Table (Model # V730-335B) and a DVC 48 digital vibration controller with four channels. The electronics stack also houses the LDA DPA K Series switching power amplifier. The computer uses DVC 48 Version 5.0 Beta software to interface the user and the controller. For this particular vibration test, the team used three ENDEVCO piezoelectric accelerometers (Model # 7221). These accelerometers should be torqued to 2.0 in-lbs. The team also used one ENDEVCO piezoelectric accelerometer (Model #2222C), which was attached to the test article using wax. The placement of these accelerometers is depicted in Figure 3.8.

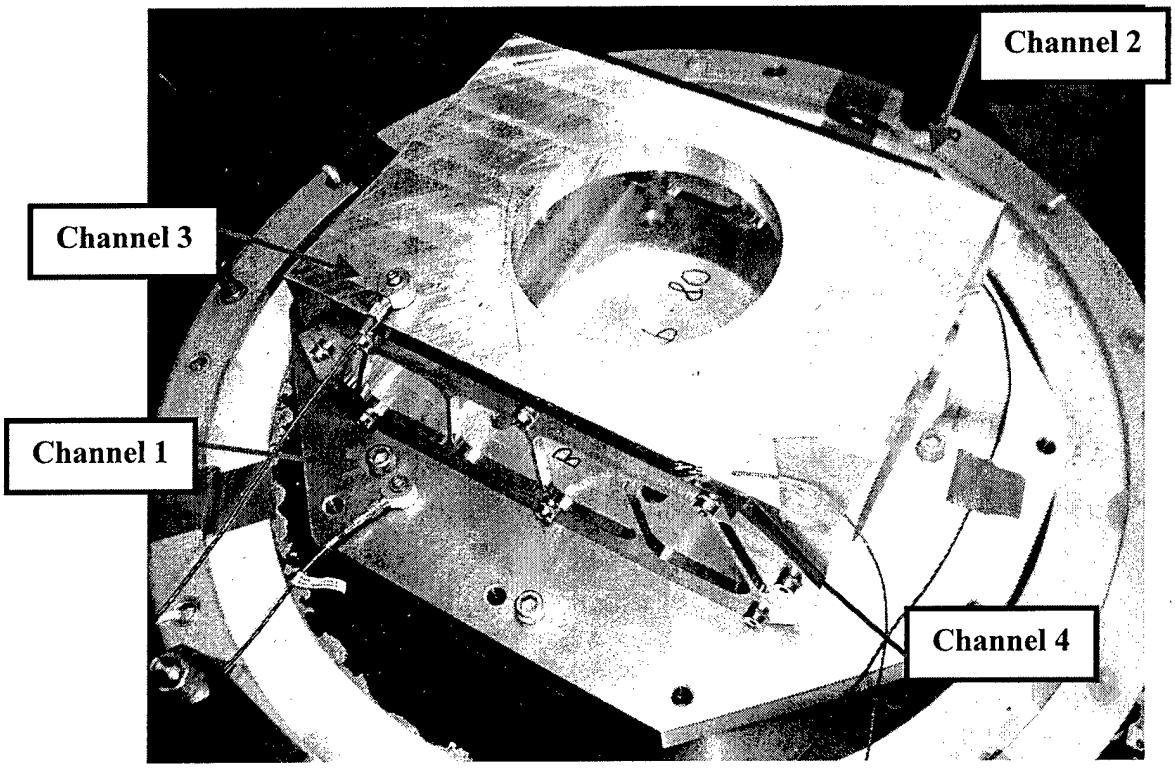

FIGURE 3.8: Accelerometer placement.

Table 3.3 shows the details of the accelerometers and their respective calibration dates.

TABLE 3.3: Accelerometer calibration and model information.

Channel	Mode	Model	Serial Number	Sensitivity	Cal Due
1	Control	ENDEVCO 7221	AAYN4	12.07 pC/pkg	9/11/04
2	Monitor	ENDEVCO 7221	AAYW1	11.37 pC/pkg	9/11/04
3	Monitor	ENDEVCO 7221	AAYN2	12.5 pC/pkg	9/11/04
4	Monitor	ENDEVCO 2222C	30193	1.492 pC/g	Date of Cal: 2/10/03

3.6 Test Procedures

In order to check that the vibration equipment is working and to verify the fundamental frequency of the base plate, a sine sweep on the base plate was conducted by Andrew Carlson. This sine sweep was accomplished from 5-2000 Hz at an input of 1.0 gn. Figure 3.9 shows the base plate mounted on the vibration table. It also depicts the attachment points of the accelerometers that were used to determine the resonance.

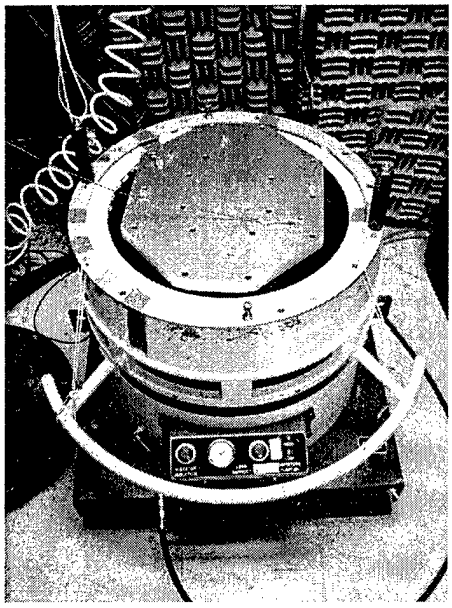

FIGURE 3.9: Vibration of the aluminum base plate.

After the successfully completion of this initial test, the base plate will be removed from the shaker table and bolted (torqued) to the vibration fixture (housing, strut plates, and reflector) and

then reattached to the shaker. The bolts attaching the vibration base plate to the vibration fixture and the vibration base plate to the shaker table should be torqued to 420 in-lbs. Figure 3.10 shows the vibration fixture bolted to the base plate, which is bolted to the shaker table.

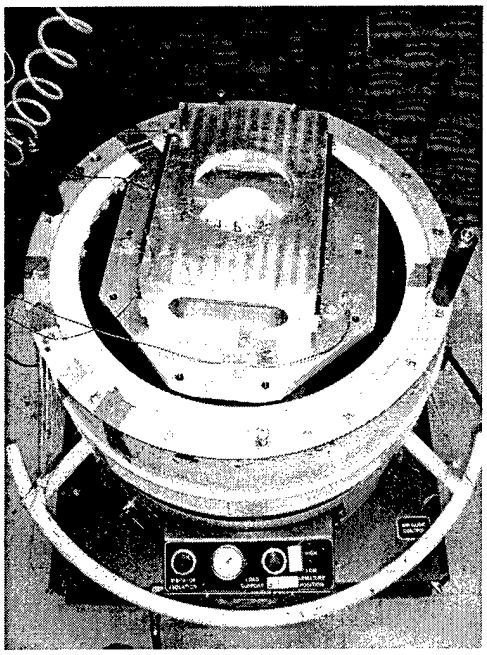

FIGURE 3.10: Test article mounted on the shaker table.

Following the sine sweep of the base plate, a sine sweep of the entire configuration (base plate and vibration fixture) should be accomplished from 5-2000 Hz at an input of 1.0 G. Predicted results determined by the analysis of Janet Squires state the first mode is present at 168 Hz and the resulting failure is predicted at 46.2 gn. This assumes that there is no preload in the reflector and that the strength of the glass is at 8.5 ksi, which was based on the strength results of the 2003 glass strength tests.

As previously stated, this particular test will forgo the random vibration test for two primary reasons. First, the goal of this test is to determine at what g-level the glass will fail. Secondly, it will be difficult to determine if defects were introduced during the random vibration test and would therefore lessen the failure load of the reflectors. Eventually a random vibe test

will be needed, but it is important to first have a clear picture of the fracture point of the glass. A sine burst test will be accomplished at a target frequency of 25 Hz (20ms/pulse) and will ramp up at levels of -12 dBs for 10 cycles, -6 dBs for 5 cycles, -3 dBs for 5 cycles, and at 0 dBs for 100 cycles. The maximum g's attempted will be less then 68.3 gn, with a shaker limitation of 75.8 gn. The 68.3 gn limitation allows for a 10% safety zone. Janet Squires, using glass strength of 8.5 ksi established in previous strength tests, predicted the failure point of the reflector to be 46.2 gn. Table 3.2 shows the planned test levels and the number of pulses at each level during the ramp up to the target load.

TABLE 3.4: DVC 48 ramp up to the predicted failure point.

Decibel Level	Gn	Pulses
-12	~11.5	10
-9	~16.5	5
-6	~23	5
-3	~32.5	5
0	~46	100

When accomplishing a test to failure using a ceramic material, it is helpful to understand the effects that fatigue has on the glass. It is therefore important to limit the time under stress at any level other than that by which is in interest. That is why the test team first attempted to reach the predicted failure point of the glass and then after the reflector survived, sought to meet the limits of the shaker table. The frequency of the test will be constantly monitored in order to ensure it is well below the fundamental frequency of the base plate and vibration fixture.

After completing the sine burst test to failure, an additional sine sweep is accomplished to determine if modes shifted indicating some sort of structural degradation in addition to the broken glass. The effects of the reflector on the fundamental frequency may be limited, since it is extremely thin and light in comparison to the rest of the test fixture.

CHAPTER 4

RESULTS AND ANALYSIS

The test team ran a successful sine sweep of the article (reflector 489 P-80). The first mode of the structure is at 600 Hz, well above that which was predicted by the analysis of Janet Squires. The reason for this is no accelerometers were placed on the face of the glass due to the expectation that this could influence the fracture outcome. Also, the mass of the reflector is much less than the mass of the vibration fixture. In future tests it is recommended that a laser vibrometer be incorporated into the test loop, so that the modal properties of the glass may be verified. The results of the sine sweep are seen in Figure 4.1 below.

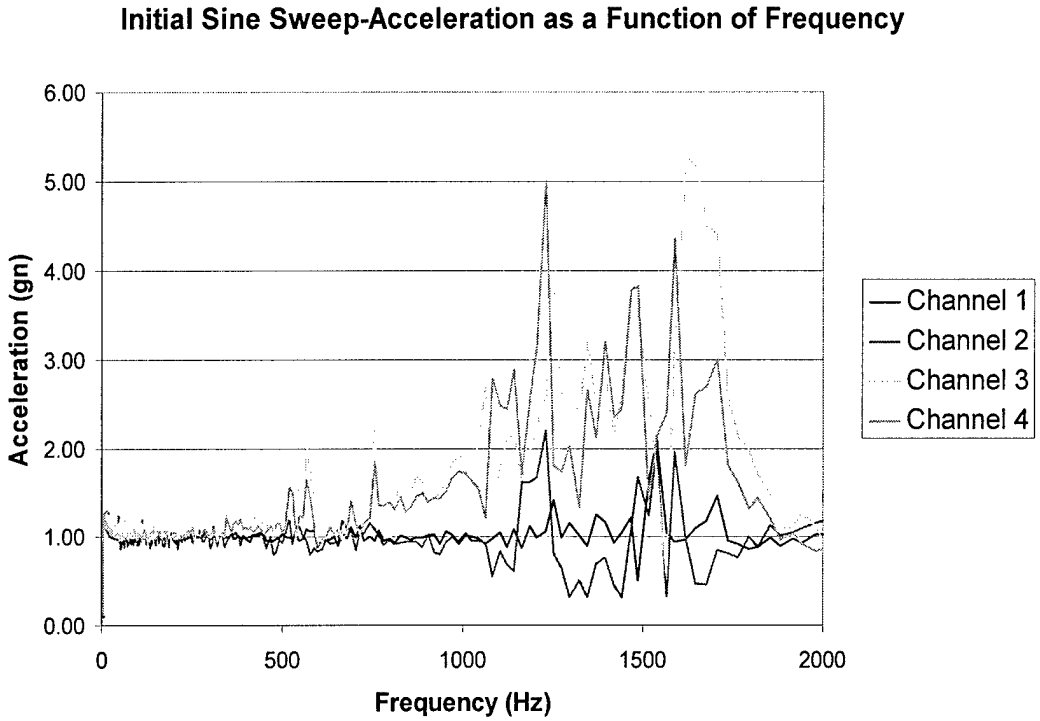

FIGURE 4.1: Pre test sine sweep of the test article.

Following the pre test sine sweep, a shock test to 46 gn was attempted. The test aborted at 26.33 gn. The team noticed that an accelerometer loosened and that is what probably resulted in the vibration table exceeding pre-defined alarm and abort limits. After hand tightening the

accelerometers, the team was able to reach a level of 45.76 gn. The glass still did not fail. At this point the team decided to test to the limits of the table and reached 75.76 gn, which is seen in Figure 4.2 below.

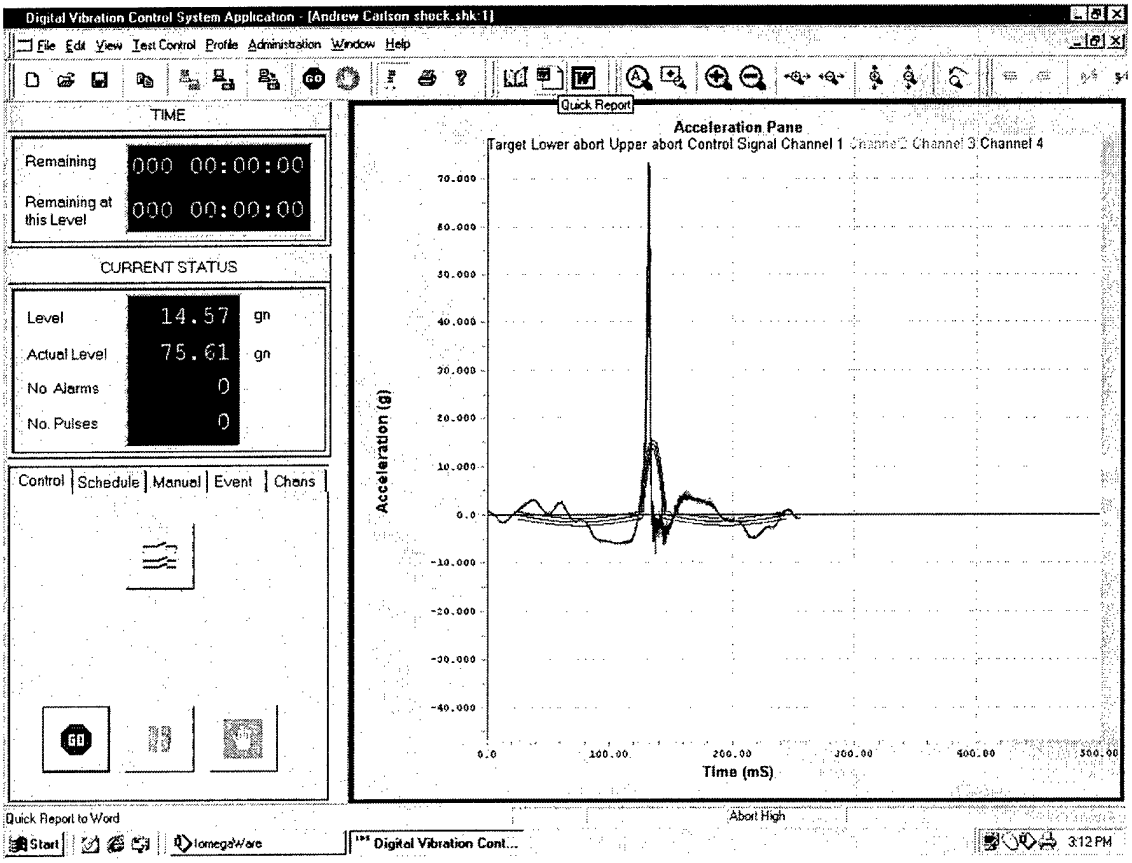

FIGURE 4.2: Results of the 75.61 gn sine burst test.

The fact that the reflector survived was a surprise to the test team at both an intuitive and analytical level. At this point shock testing was ended as the table limits were met.

Following the shock testing, a post shock sine sweep was accomplished to check for structural damage. The first mode and acceleration of the post test sine sweep are at 600 Hz and 2.0 gn, similar to the pre test sine sweep results. Other departures in the data however exceeded the pre test sine sweep results by about 1 gn at the frequency range greater than 1200 Hz.

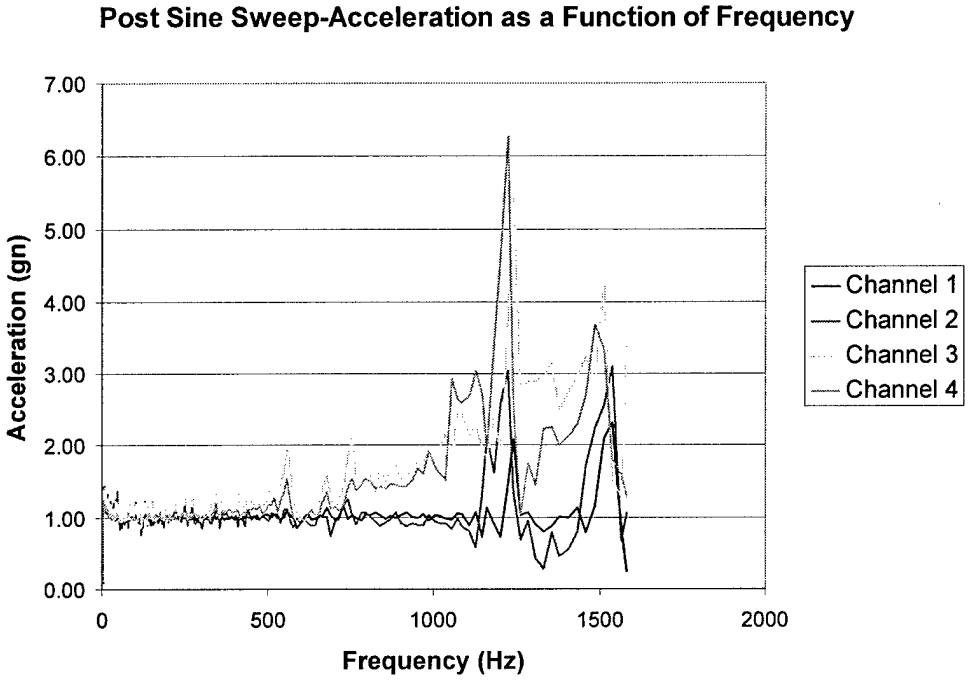

FIGURE 4.3: Post test sine sweep of the test article.

Figure 4.3 shows the results of the post test sine sweep. It is clear that there is a difference between the acceleration peaks of the pre and post sine sweep charts especially in the higher frequency range around 1250 Hz. As previously stated, following the 26.33 gn shock test, it was noticed that the Channel 3 accelerometer may have loosened during the initial sine sweep and the 26.33 gn shock test. The Channel 1, 2, and 3 bolts were then hand tightened to a torque value greater than 2.0 in-lbs, which held the accelerometers in place for the remainder of the shock testing and post test sine sweep. This tightening may have caused this shift in acceleration levels, which is apparent in the acceleration feedback of all four channels. It should also be noted that Channel 4 was attached by wax and therefore it may be a possibility that some component may have loosened, which would affect the entire fixture (including the base plate). This would most likely isolate an issue with the base plate and shake table interface. The team did know prior to test that aluminum does not have the most favorable damping qualities.

Following the post test sine sweep, a visual inspection revealed no signs of structural degradation or fatigue. No visible defects or cracks were found in the reflector. When disassembling the article from the shaker, all bolts seemed tight.

Table 4.1 summarizes the tests that were accomplished on the reflector.

TABLE 4.1: History of sine sweeps and shock tests.

Test Type	Level
Pre Test Sine Sweep	5-2000 Hz @ 1gn
Shock Test	26.33 gn
Shock Test	45.76 gn
Shock Test	75.76 gn
Post Test Sine Sweep	5-2000 Hz @ 1 gn

The team cannot be certain what caused the shift in acceleration data between the sine sweeps. As previously stated, no visible degradation occurred within the fixture or reflector. Overall this is a very successful test and despite that fact that it is only one data point, the news is exciting for the Constellation X program.

CHAPTER 5

CONCLUSIONS

This thesis provided a general background into the mission and science behind Constellation X. The mission is the key to answering questions about the mysterious properties of black holes, dark matter, and other celestial events. In any project, an appreciation for the overall mission and goals will most likely result in added intrinsic value to work accomplished on a smaller scale. The problems of any program seem important when their effect on the overall mission is understood. In addition, much research was accomplished in the areas of ceramic properties and glass strength. Glass strength is one of the key variables used in the finite element analysis models. Unfortunately, large scatter in ceramic data results in a variable that is least understood. It should be noted that present testing is being accomplished to paint a better picture of glass strength and to isolate the variables and procedures, which in fact may decrease the strength. Analysis was accomplished to determine that the current mounting of the glass provides a negative margin of safety on the spacecraft component. Vibration standards and techniques were evaluated through research into NASA Specs and Aerospace literature.

A major portion of this thesis was the challenge of designing a test that would accurately simulate the boundary conditions of the launch environment. The NASA Con-X SXT Mechanical Systems Engineering Team worked through this entire process. The team designed a vibration fixture, ran a thermal analysis on the fixture, machined and assembled the fixture, and then ran structural analysis to predict fundamental frequencies and the failure point of the reflector. The results of this work were a comprehensive test plan explaining assembly procedures, test procedures, and procedures regarding data reduction. Overall, this was the most work intensive and difficult portion of the project.

The original test plan consisted of a pre shock sine sweep, shock test, and post shock sine sweep. The 1st mode of the fixture was present at 600 Hz. This of course is not the first mode of the reflector, which is predicted to be much less. Additional instrumentation such as a laser vibrometer will need to be incorporated to determine this modal information. The first shock test aborted at 26.33 gn, the second test achieved 45.76 gn, and the last test reached 75.61 gn. The reflector survived a load of 75.61 gn. This is well above the failure point predicted by the team's models, which was 46.2 gn. The last test was taken to the maximum capability of the shaker table and therefore another vibration facility is warranted.

When this reflector is vibrated to failure, it is important to remember that this is merely one data point. The results of this test alone will not provide enough information by which to hone the glass strength value used in analytical models, but the results of multiple tests should reduce scatter in the data. NASA Goddard's vibration test facility does have a laser vibrometer and the modal information obtained during the sine sweep using this equipment should be accurate enough to correlate with the models. As previously explained, the use of this facility is fairly expensive, which was the reason the Building 5 LDS shaker table was used in the first place. The test team however feels that now is the time to push the program for additional funds for more complex and capable vibration testing since the limits of the Building 5 LDS shaker table have been reached.

Overall, this has been a very successful test. The test developed by the NASA Con-X SXT Mechanical Systems Engineering Team will prove invaluable to further testing accomplished. The fixture and procedures are transferable to any testing that will be accomplished in NASA Goddard's main vibration test facility. The development of this test is another success in NASA's distinguished list of achievements.

CHAPTER 6

FUTURE DIRECTION

This thesis incorporates one vibration test of one sample. The reflector survived a load of 75.61 g's, which is also the limit of the shaker table. The next step is to vibe the reflector on a more capable shaker table that will take the reflector to failure. Now that the test fixture is designed, manufactured, and assembled and test procedures are established, multiple data points must be obtained to reach statistically validated conclusions. Many variables exist, such as environmental factors, quality of glass, type of defects which result in failure, and the location of these defects. Some ideas to isolate a few of these questions include placing Kapton tape on the back of a reflector in order to hold the shards of glass together and to isolate the fracture origin. Additional studies should be made to understand the effects that Kapton tape will have on the failure point of the glass during a dynamic test. Future tracking of test samples from delivery to test should be accomplished to ensure the defects introduced are minimized. After a clear understanding of the behavior of glass in a dynamic environment, further tests should validate alternate methods of mounting the glass. Instead of grooves in struts and an epoxy interface between the glass and titanium, other ideas include foam insulation, attachment to piezo, and Teflon insulation. The incorporation of a laser vibrometer into the system should provide very precise data regarding the natural frequency, fracture point and time that it took place.

REFERENCES

[1] The Constellation X-ray Mission TRIP (Technology Readiness and Implementation Plan) Site Visit Briefing. 20 March 2003.

[2] Constellation X Comparison of Constellation Spectrometer Effective Area with Previous Missions. <http://constellation.gsfc.nasa.gov/images/area-res.jpg>. 19 Dec 2003.

[3] Constellation X Reference Design. <http://constellation.gsfc.nasa.gov/docs/design/images/slide01.tif>. 19 Dec 2003.

[4] SXT FMA Industry Study Pre-Bidder's Conference. <https://conxproj.gsfc.nasa.gov/business/busdocs/Pre-Bid_Final_onefile_11-13-03.pdf>. 5 Nov 2003.

[5] Technology Spectroscopy X-Ray Telescope. <https://constellation.gsfc.nasa.gov/science/technology/sxt.html>. 3 Aug 2004.

[6] Squires, Burt. SXT Technical Interchange Meeting (TIM) Reflector Strength and Alignment. 10 Dec 2003.

[7] Joy, Pilar T. Characterization of SCT Segments Optics Test Plan. NASA-GSFC-541. 4 Dec 2002.

[8] Bansal, Narottam P. and Doremus, R. H. Handbook of Glass Properties. New York: Academic Press, Inc., 1986.

[9] Villani, Angelo. "A square ring on square ring (SoS) ceramic strength testing

technique for VLSI packaging. Microelectronic Reliability." Elsevier Science Ltd. 2000.

[10] Varshneya, Arun K. Fundamentals of Inorganic Glasses. San Diego: Academic Press, Inc., 1994.

[11] Schott Glass. <http://www.schott.com/fpd/english/products/fpd/d263t.html#main>. 2003.

[12] He, Charles. Strength of slumped Glass Shells for Constellation X. 17 Dec 2003.

[13] He, Charles. Constellation X Glass Strength Investigation Strength Variation Among Deliveries and Effect of Cleaning on Strength. 23 June 2004.

[14] Chung, Y.T., Krebs, D.J., and Peebles, J.H. Estimation of Payload Random Vibration Loads for Proper Structure Design. AIAA-2001-1667. April 2001.

[15] Goddard Space Flight Center. General Environmental Verification Specification (GEVS) for STS and ELV Payloads, Subsystems, and Components, Revision A. <http://arioch.gsfc.nasa.gov/302/gevs-se/toc.htm>.

[16] Branstetter, Linda J., Gregory, Danny L., and Paez, Thomas L. "Random Variation of Modal-Frequencies-Experiment and Analysis." Testing Techniques. Sandia National Laboratories. Albuquerque, New Mexico.

[17] Chen, Jay-Chung and Womack, J.R. Structural Evaluations and Dynamic Testing of Solar Electric Propulsion Components. AIAA 72-442. April 1972.

[18] Barnes, Donald A. and Pontius, James T. Structural Qualification of a Spacecraft Payload Using Near-Resonance Sine Burst Testing. AIAA 2003-1452. April 2003.

[19] Squires, Janet. Constellation X SXT Reflector Vibration Analysis. 17 Aug 2004.